A NOVEL BIOSENSER FOR HYDROGEN PEROXIDE BASED ON HORSERADISH PEROXIDASE IMMOBILISED ON A ZINC OXIDE-MULTIWALLED CARBON NANOTUBE COMPOSITE

BY

BONITA CHENGETAI NYAWO

(R131717A)

Submitted in partial fulfillment of the requirements for the degree of

Bachelor of Science Honours in Chemical Technology

Department of Chemical Technology

in the

Faculty of Science and Technology

at the

Midlands State University

Supervisor: Dr. M. MOYO

November 2016

DEDICATION

I dedicate this work to my family and friends.

ACKNOWLEDGEMENTS

I would like to thank God for making this project possible for me, the good learning environment I had and the individuals that assisted me through their moral, financial, technical support, critique and personal commitment as they made my project viable. My gratitude also goes to Dr Moyo for his efforts, contributions, sharing insights, guidance and infinite patience in writing this research. Equal thanks go to the laboratory staff of Midlands State University Chemical Technology for its support. I want to thank my family who supported me financially and emotionally throughout the project.

ABSTRACT

A novel biosensor for hydrogen peroxide was constructed based on the immobilization of horseradish peroxidase on zinc oxide-multiwalled carbon nanotubes matrix. The model redox enzyme, horseradish peroxidase (HRP) was physically (physical adsorption) immobilized on the ZnO/MWCNT modified electrode surface. UV-Visible spectra of HRP and HRP/ZnO/MWCNT displayed soret bands at 407 and 390 nm, respectively and thus the immobilised HRP retains its native structure. The modified electrode was characterised by cyclic voltammetry and electrochemical impedance in a redox probe. The surface area of the electrode after modification was 0.123cm^2, which was almost twice as that of a bare glassy carbon. The fabricated sensor was applied for the detection of hydrogen peroxide. The LOD and LOQ were found to be 3.48×10^{-7} M and 1.05×10^{-6}M, respectively. The sensor displayed good reproducibility and stability for the detection of hydrogen peroxide.

DECLARATION

I, Bonita Chengetai Nyawo R131717A, hereby declare that I am the sole author of this dissertation. I authorize Midlands State University to lend this dissertation to other institutions or individuals for the purpose of scholarly research.

Signature ……

Date …….

APPROVAL

This dissertationentitled, "*A novel biosensor for hydrogen peroxide based on horseradish peroxidase immobilized on a zinc oxide-multiwalled carbon nanotube composite*" by……. meets the regulations governing the award of the degree of……..……..……... of the Midlands State University, and is approved for itscontribution to knowledge and literal presentation.

Supervisor ……

Date …….

TABLE OF CONTENTS

LIST OF FIGURES

LIST OF TABLES

.

ABBREVIATIONS

CV- Cyclic voltammetry

MWCNT- Multiwalled carbon nanotubes

DPV- Differential pulse voltammetry

EIS- Electrochemical impedance spectroscopy

GCE- Glassy carbon electrode

LOD- Limit of detection

LOQ- Limit of quantification

IEP-Iso-electric point

WE- Working electrode

RE- Reference electrode

CE- Counter electrode

PBS- Phosphate buffer solution

UV-Vis- Ultraviolet visiblespectroscopy

HRP-Horseradish peroxidase

GC- Gas chromatography

TLC- Thin layer chromatography

LA- Lauric acid

HOPG- Highly oriented pyrotic graphite

DNA- Deoxyribose nucleic acid

CHAPTER ONE

1.0 Introduction

The present chapter serves to highlight the background of the research and the other techniques/methods that were used for the sensing of hydrogen peroxide. The problem statement and justification of the study are also discussed.

1.1 Background

Hydrogen peroxide (H_2O_2) is one of the most multifaceted of the existing oxidizing agents. It plays an essential role in the regulation of several biological processes. These include the defense mechanism to the immune system and cell growth regulation [1]. The interest in hydrogen peroxide detection is linked to its environmental, clinical and industrial applications. The interest is also due to the increased awareness of environmental hazards and the need for safe detection procedures [2]. This range of applications has encouraged for the intensive studies for fast and accurate hydrogen peroxide determination techniques at very low concentrations [3].

The use of nanostructured materials in electrochemistry has increased over the past years as nanomaterials seem to be promising matrices for enzyme immobilization due to their large specific surface area, excellent conductivity and biocompatibility and suitable mechanical and thermal properties [4]. The chemical modifications of bare electrodes with a thin film of a suitable electroactive species offer remarkable advantages in the design and development of electrochemical sensors and biosensors. In practice, electrode surface modification has been used as a means of reducing overvoltage and overcoming the slow kinetics of many electrode processes [5].

As widely used nanostructures, carbon nanotubes are very promising materials for electrode modification as a result of their unique electronic and mechanical properties including high conductivity, electro catalytic effect, high surface area and chemical stability [6]. Carbon nanotubes catalyze redox reactions of different analytes; moreover, it is possible to immobilize biomacromolecules such as enzymes and DNA, which allows the development of sensors [7].

In addition to carbon nanotubes, other valuable, important electrode materials are the metal oxides which have attracted great interest as of recent years because of their use in catalyst supports. As a metal oxide, Zinc oxide (ZnO) nanostructures have excellent physiochemical properties including high surface area, low toxicity and can be easily prepared, lowering costs of the analysis. ZnO has also gained special attention due to its wide band cap, semiconducting and piezoelectric properties. It also has a high iso-electric point (IEP~9.5), which facilitates the adsorption of negatively charged HRP enzyme at physiological pH [8].

Horseradish peroxidase is a heme containing enzyme and has high stability and bioactivity towards H_2O_2. It is used due to its ability of amplify weak signals and increase the detectability of a target molecule. Its presence is made visible by using a substrate that when oxidized by HRP using hydrogen peroxide as an oxidizing agent, yields a characteristic change that is detectable by spectrophotometric methods [9].

1.2 Aim:

To fabricate a hydrogen peroxide sensor by immobilization of Horseradish peroxide on zinc oxide/ multiwalled carbon nanotubes deposited on glassy carbon electrode.

1.3 Objectives:

- To synthesize zinc oxide nanoparticles.
- To monitor activity of the enzyme using the UV- vis Spectroscopy.
- To modify the bare electrode with multiwalled carbon nanotubes, zinc oxide and horseradish peroxidase using the drop dry method.
- To characterize the modified electrodes using cyclic voltammetry and electrochemical impedance in a redox probe.
- To evaluate the effect of different pH and scan rate on the peak currents and potentials in 0.1M phosphate buffer.
- To study the direct electrochemistry of HRP in 0.1 M phosphate buffer.
- To study the effect of different modified electrodes on the electro catalytic redox of hydrogen peroxide using cyclic voltammetry.
- To study the impedemetric effect of the modified electrode on the redox reaction of hydrogen peroxide
- To determine the electrode transfer kinetics, Tafel slopes, catalytic rate constants and relative catalytic effects of the modified sensor.
- To calculate the detection limit of the HRP/ZnO/MWCNT/GCE on hydrogen peroxide
- To study the stability and reproducibility of the developed electrode towards the reaction of hydrogen peroxide

1.4 Problem statement

It is often proposed that the toxicity of many drugs and chemicals results from excessive generation of superoxide (O^{2-}) and H_2O_2, perhaps by exceeding the capacity of cellular enzyme systems to remove them efficiently [10]. Reactive oxygen intermediates maybe generated in the lungs during various pathological processes. These intermediates and H_2O_2 itself are toxic to cells due to their oxidizing effects. These peroxide levels can damage mammalian cells.

In electrochemistry, hydrogen peroxide can either be oxidized or reduced directly at ordinary solid electrodes. The use of these electrodes, such as Pt electrodes, is widespread in the construction of sensors, which are normally based on amperometric detection. However, this kind of electrode is limited by slow transfer kinetics and high over potentials, which compromise the sensing performance and may suffer interference from other electroactive species in the real sample [11].

Currently, various methods have been successfully applied in the construction of Hydrogen peroxide sensors such as Nafion film [12], Prussian blue [3], metal oxides [13] and redox polymers. However, these devices require several selective coatings layers, which lead to increased response times due to the limiting step of analyte diffusion through the deposited layers and its expensive [14].

Generally, direct electron transfer between HRP and an electrode is difficult because the active sites of HRP are deeply buried in a thick protein shell, and because the large distance between the active sites and the electrode surface will slow down the electron transfer [8].

1.5 Justification

Many methods have been proposed to determine hydrogen peroxide including titrimetry, spectrophotometry, chemiluminesescence, chromatography, iodometry, and electrochemical methods. However, most of these methods require extensive or laborious chemical reactions, prior purification, expensive facilities as well as limitations conditions in terms pH, conductivity and the presence of the interfering compounds.In contrast, electrochemical methods require only limited instrumentation while providing high precision data over short time periods[15]. Additionally, detection can be performed through analyte oxidation or reduction: allowing for application of a greater range of chemical systems. Further, electrochemical methods can be performed to monitor changes in current (amperometric), voltage (voltammetric), or impedance (electrochemical impedance)[16].

Novel analytical devices based on nanostructured metal oxides arecost-effective, highly sensitive due to the large surface-to-volume ratio of the nanostructures, andadditionally show excellent selectivity when coupled to biorecognition molecules with simple design [17]. Multiwalled carbon nanotubes and zinc oxide composite are associated with low toxicity, can be easily prepared, hence lowering the cost of analysis. They are economic and environmental-friendly materials hence their use in this research. Since hydrogen peroxide is an electroactive molecule, electrochemical techniques have attracted much attention based on their high sensitivity, specificity, speed, portability and low cost [18].

CHAPTER 2

LITERATURE REVIEW

2.0 Introduction

The present chapter gives an outline of hydrogen peroxide, electrochemical sensors, horseradish peroxidase, multiwalled carbon nanotubes, zinc oxide nanoparticles, and all the theory of electrochemistry techniques used in this study.

2.1 Hydrogen peroxide

Hydrogen peroxide is a clear and colorless liquid with a slight pungent odor at room temperature. Small amounts of gaseous hydrogen peroxide occur naturally in the air. Although nonflammable, it is a powerful oxidizing agent that can cause spontaneous combustion when it comes in contact with organic material [19]. It is among the strongest oxidizing agents and can be a reducing agent for strong oxidizers. Hydrogen peroxide is unstable, decomposing readily to oxygen and water with release of heat. Because the decomposition products of hydrogen peroxide are water and oxygen, hydrogen peroxide is preferred for many applications [20].

Hydrogen peroxide is a known molecule with many useful applications in pharmaceuticals, the medical field, and the food and textile industries [21]. In nature it is the byproduct of many oxidase enzymes, that when reacting with their specific substrate produces it. These oxidase enzymes are glucose, oxidase, lactose oxidase among others [22]. Furthermore, in living organisms, in addition to its well known cytoxicity effect, hydrogen peroxide concentrations greater than 50 μM causes damage to the DNA and lipids in the cell wall [23]. Hydrogen peroxide plays an important role as signaling molecule in diverse processes, such as cell immune activation, vascular remodeling and apoptosis[23]. It is a strong oxidizing agent that is extremely

attractive for the development of new technologies. Since it is a very important molecule in many processes, a robust, stable, reliable, reusable and accurate sensor for the determination of hydrogen peroxide to this date is of extreme importance.

2.1.1 Hydrogen peroxide sensor

Different techniques have been used for the detection of hydrogen peroxide and these include titrimetry , spectrophotometry [24] and Chemiluminescense [25]. Electrochemical methods have attracted considerable interest due to their high sensitivity, fast response, low cost and convenient operations [5]. Generally electrochemical sensors can be subdivided into groups i.e. a sensor and a biosensor.

Sensors are devices which are composed of an active sensing material with a signal transducer. The role of these two important components in sensors is to transmit the signal without any amplification from a selective compound or from a change in a reaction [17]. These devices produce any one of the signals as electrical, thermal or optical output signals which could be converted in to digital signals for further processing. One of the ways of classifying sensors is done based on these output signals [26]. Among these, electrochemical sensors have more advantage over the others because; in these, the electrodes can sense the materials which are present within the host without doing any damage to the host system.

Biosensors can be defined in terms of sensing aspects, where these sensors can sense biochemical compounds such as biological proteins, nucleotides and even tissues [17]. Within these sensors, the active sensing material on the electrode should act as a catalyst and catalyze the reaction of the biochemical chemical compounds to obtain the output signals [27]. The combination of these two different ways of classifications has given rise to a new type of sensors

which are called electrochemical biosensors, where the electrochemical methods are applied for theconstruction and working of a biosensor

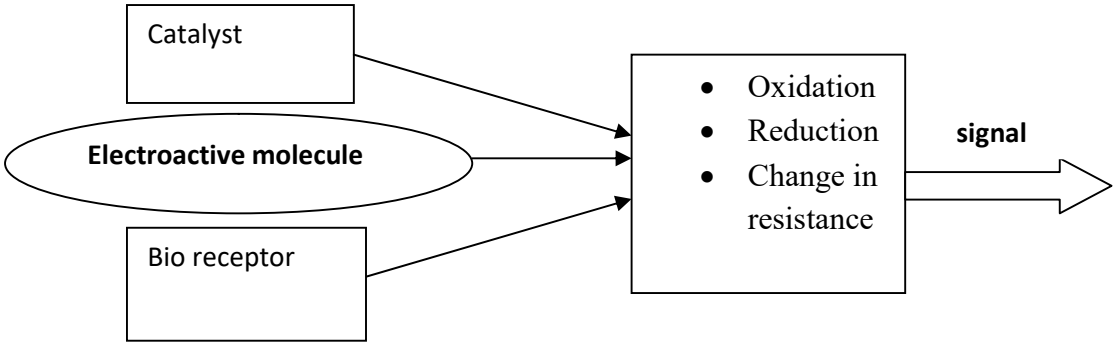

Fig 2.1: Schematic representation of an electrochemical biosensor

Fig 2.1 shows a schematic presentation of an electrochemical biosensor, where a bio-receptor is immobilized at the catalyst surface. Most common bio-receptors are nucleic-acid interactions, cellular interactions and interactions using biometric interactions [28]. For a bio-receptor whose reaction produces an electroactive molecule (H_2O_2 or mediator), the latter can be oxidized or reduced at the electrode surface. The current measured will correlate with the concentration of the analyte in solution and a calibration curve can be plotted [29].

If the bio receptor does not produce an electroactive molecule, electrochemical impedance spectroscopy technique can be used to follow the reaction with a change in resistance at the electrode surface. The change in resistance will then correlate with the concentration of the analyte in solution and a calibration curve can be plotted [30]. In a sensor, an electroactive molecule is oxidized or reduced at the electrode surface, a change in current is measured and plotted to develop a calibration curve.

In the case of hydrogen peroxide, the sensors are classified into two main groups i.e. enzymatic and non enzymatic sensors. The following reactions summarize the oxidization and reduction of H_2O_2 at the surface of the electrochemical sensor

Oxidation reaction

$$H_2O_2 \longrightarrow O_2 + 2H^+ + 2e^- \qquad (2.1)$$

Reduction reaction

$$H_2O_2 + 2e^- + 2H^+ \longrightarrow H_2O \qquad (2.2)\ [24]$$

Different materials have been used for the detection of hydrogen peroxide from carbon-based, inorganic material, polymers e.t.c. [31]. In the research, carbon nanotubes and zinc oxide were used as the immobilization matrix for horseradish peroxidase.

2.2 Horseradish peroxidase

HRP is one of the most extensively studied and mostly usedenzymes for the construction of H_2O_2 biosensors[8]. It contains heme as a prosthetic group, which is the protein active site, along with the hemeiron Fe (III). It can catalyze the oxidation of a wide variety of substratesby H_2O_2. Moreover, the reduced form of HRP can be chemically reoxidized by H_2O_2. Generally, direct electron transfer between HRP and an electrode is difficult because the active sites of HRP are deeply buried in a thick protein shell, and because the large distance between the active sites and the electrode surface will slow down the electron transfer[5].

Direct electron transfer between enzymes and electrodes is not easy and therefore, need to use mediator. Electron transfer via a mediator, however, is more effective for establishing an

electrical connection between the redoxcenters and the electrode[32]. The role of the mediator is to shuttle electrons efficiently between electrode and enzyme. In the presence of mediator (M), the reaction mechanism of the H_2O_2biosensor based on the HRP enzyme modified electrodes can be summarized as follows [33].

$H_2O_2+HRP_{red} \rightarrow H_2O+HRP_{ox}$(2.3)

$HRP_{ox}+M_{red} \rightarrow HRP_{red}+M_{ox}$ (2.4)

$M_{ox}+2H^{+}+2e \rightarrow M_{red}$(2.5)

Net reaction: $H_2O_2+2e+2H^{+} \rightarrow 2H_2O$(2.6)

First, H_2O_2 in the solution is reduced by the immobilized HRP. Then the reduced HRP is regenerated with the aid of the mediator, while the mediator itself is oxidized in the enzymatic reaction. Finally, the oxidized mediator is electrochemically reduced on the electrode, leading to an increase in the reduction current.

2.2.1 Mediator-free HRP based biosensor

The direct electrochemical behavior of the enzyme or protein atthe electrode surface provides a foundation for the fabrication of themediator-free biosensors. It simplifies the preparation processes ofsensing devices and avoids the toxicity of the mediator, in comparisonwith the mediator based biosensors. It features the advantages of highsensitivity and selectivity, and therefore, attracts considerable attention [34]. Depending on the immobilizing matrix, HRP exhibits directelectrochemical behavior towards the reduction of H_2O_2. For example,

..

a quasi-reversible electron transfer was observed in the absence of mediator, when HRP is incorporated in a salt bridge-supported BilayerLipid Membrane (sb-BLM), modified with Lauric Acid (LA)[35]. Zhanget al. (2006) utilized this quasi-reversible electron transfers to construct a H_2O_2 biosensor[36].

Different nanomaterials are widely used for the development ofmediator-free HRP enzyme based biosensor. Liu and Ju (2003) proposeda renewable reagentless H_2O_2 biosensor based on the direct electron transfer of HRP, which was immobilized on a gold nanoparticle-modified carbon paste electrode[37]. Electrochemical methods were used to investigate the direct electrochemistry of HRP. The biosensordisplayed an excellent electro catalytic response to the reduction ofH_2O_2, without the aid of an electron mediator. Gold nanoparticles modified ITO electrode was also used for the immobilization ofHRP and investigation of the direct electrochemistry of HRP [36]. However, the performance of the mediator-free biosensor increasedwhen gold nanoparticles and HRP embedded simultaneously on sol–gel network [38]. Yin et al.(2009) reported the preparation of HRP–Gold Nanoparticles (GNPs)–Silk Fibroin (SF) modified GCE by one step procedure, and investigated the direct electrochemistry of HRP at the modified electrode[39]. The fabricated mediator-free biosensor showed an excellent and quick electrocatalytic response to the reduction of H_2O_2.

2.2.2 Immobilization of horseradish peroxidase

As enzymes are biological catalysts that promote the rate of reactions but are not themselves consumed in the reactions; they may be used repeatedly for as long as they remain active. However, in most of the processes, enzymes are mixed in a solution with substrates and cannot be economically recovered after the reaction and are generally wasted [40]. Thus, there is an incentive to use enzymes in an immobilized or insolubilized form so that they may be retained in

a biochemical reactor for further catalysis. This is done by enzyme immobilization which may be defined as the process whereby the movement of enzymes, cells, organelles, etc. in space is completely or severely restricted usually resulting in a water-insoluble form of the enzyme [41]. There are different methods for immobilization, such as entrapment, physical adsorption and covalent binding.

2.2.2.1 Entrapment

The entrapment method consists in art of the immobilization of n enzyme in polymer or membrane matrix. The basic concept is retaining the protein while allowing penetration of the substrate [42]. In entrapment, the enzymes or cells are not directly attached to the support surface, but simply trapped inside the polymer matrix. Entrapment is carried out by mixing the biocatalyst into a monomer solution, followed bypolymerization initiated by a change in temperature or by a chemical reaction.The disadvantage of this method is that enzyme can leak into the surrounding medium.Another problem is the mass transfer resistance to substrates and products [42].

2.2.2.2 Physical adsorption

This method is the easiest. It is based on a direct adsorption of the enzyme on a surface matrix. This method is achieved via Van der Waals forces, ionic binding or hydrophobic forces that allow the enzyme to be attracted and adsorb on the surface. The advantages of this method are that it is simple, requires a minimum of steps and causes little conformational changes on the analyte. However, because the enzyme is not strongly held on the surface matrix, the disadvantage is that the enzyme may leach from the matrix due to changes in temperature, pH, ionic strength or even the presence of the substrate [43]. This method is the one that was used in

this research because it causes little or conformational changes to the enzyme,simple and cheap,wide applicability and capable of high enzyme loading.

2.2.2.3 Covalent Bonding

This method is a technique based on binding of a functional group of the enzyme and the matrix via a covalent bond. This method improves uniformity, density, and distribution of the bound analyte. The conditions to perform are far more complicated than simple adsorption or entrapment in a matrix and may alter the conformational and active center of an enzyme [44].

2.2.2.4 Cross linking

This method is also called as copolymerization. In this method of immobilization enzymes are directly linked by covalent bonds between various groups of enzymes via polyfunctional reagents. Unlike other methods, there is no matrix or support involved in this method. Commonly used polyfunctional reagents are glutaraldehyde and diazonium salt. This technique is cheap and simple but not often used with pure enzymes. This method is widely used in commercial preparations and applications. The greatest disadvantage or demerit of this method is that the polyfunctional reagents used for cross linking the enzyme may denature or structurally modify the enzyme leading to the loss of catalytic properties [45].

2.3 Carbon nanotubes

Carbon nanotubes (CNTs) are allotropes of carbon with a cylindrical nanostructure. These cylindrical carbon molecules have unusual properties, which are valuable for nanotechnology, electronics, optics and other fields of materials science and technology. Owing

to the material's exceptional strength and stiffness, nanotubes have been constructed with length-to-diameter ratio of up to 132,000,000:1 significantly larger than for any other material[46].

Nanotubes are members of the fullerene structural family. Their name is derived from their long, hollow structure with the walls formed by one-atom-thick sheets of carbon, called graphene. These sheets are rolled at specific and discrete angles and the combination of the rolling angle and radius decides the nanotube properties; for example, whether the individual nanotube shell is a metal or semiconductor. Nanotubes are categorized as single-walled nanotubes (SWNTs) and multi-walled nanotubes (MWNTs). Individual nanotubes naturally align themselves into ropes held together by van der Waals forces, more specifically, pi-stacking[47].

Recently, several studies have highlighted the prospect of using carbon nanotubes as building blocks to fabricate three-dimensional macroscopic (>100 nm in all three dimensions) all-carbon devices. A novel radical initiated thermal cross linking method to fabricate macroscopic, free-standing, and porous, all-carbon scaffolds using single- and multi-walled carbon nanotubes as building blocks was reported [48]. These scaffolds possess macro-, micro-, and nano- structured pores and the porosity can be tailored for specific applications. These 3D all-carbon scaffolds/architectures may be used for the fabrication of the next generation of energy storage, super capacitors, field emission transistors, high-performance catalysis, photovoltaic, and biomedical devices, sensors and implants.

CNTs have unique mechanical and electronic properties, combined with chemical stability, and behave electrically as a metal or semiconductor, depending on their

structure. For sensing applications [49]. CNTs have many advantages such as small size with larger surface area, excellent electron transfer promoting ability when used as electrodes modifier in electrochemical reactions, and easy protein immobilization with retention of its activity for potential biosensors. CNTs play an important role in the performance of electrochemical biosensors, immunosensors, and DNA biosensors [46]. Hence, their use in this research paper.

2.3.1 Electrochemistry of carbon nanotubes

CNTs are electrochemically inert materials similar to other carbon-based materials used in electrochemistry, i.e. glassy carbon, graphite, and diamond. They possess distinct electrochemical properties because of their unique electronic structure. The carbon atoms of CNTs at the sidewall and the end of the tubes are not same and their behavior can be compared with the basal plane and edge plane of highly oriented pyrolytic graphite (HOPG), respectively [50]. Compton et al. (2004) studied the redox reaction of ferricyanide at the C60- and nanotube modified electrodes and compared these results with basal and edge planes pyrolytic graphite electrodes. They observed similar electron transfer rate constants for CNTs-modified and the edge plane HOPG electrodes. They reported that the CNTs acted as an efficient electron transfer pyrometer [51].

Considering these electronic properties, carbon nanotubes are known for their capacity of boosting electron transfer reactions and enhancing sensitivity in electro analysis[11].From research findings it has been demonstrated that use of MWCNTs can be elevated by adding other functional groups or different nanomaterials onto their surfaces. The mix of MWCNTs with different nanomaterials has been accounted to be very helpful for creating electrochemical

sensors[5]. Multi-walled carbon nanotubes have similar properties to single walled nanotubes, yet the outer walls on multi-walled nanotubes can protect the inner carbon nanotubes from chemical interactions with external materials. Multi-walled nanotubes also have a higher tensile strength than single-walled nanotube. Electrochemical characterization involving conjugates of MWCNTs and nanoparticles is expanding rapidly in electro-analytical researches because the conjugates have more appreciable electro-catalysis effect compared to the nanotube or nanoparticles alone[52].

2.4 Nano zinc oxide

Since, metal oxides possess unique advantages such as high sensitivity, good selectivity and large surface-to-volume ratio, so far increasing number of researchers have reported the production of novel CNT–metal oxide nanocomposites for biosensors applications[53], [54].To enhance the performance features of the biosensor and to efficiently immobilize enzymes onto the electrode surfaces, various nanomaterials matrices have been used. Zinc oxide (ZnO) is well known for its interesting features and has been a promising material with good biocompatibility, high surface activity, and rapid electron communication features[55]. These salient featuresof ZnO are highly advantageous for enzyme-based biosensor applications, and ZnO has been used as a potent matrix for immobilizing redox proteins successfully for efficient H_2O_2 detection [56]. Apart from these interesting aspects of ZnO, great interest has been shown toward the synthesis of MWNT/ZnO composites with interesting morphologies using versatile strategiesincluding hydrothermal[57], thermal decomposition, drop casting and electrodeposition[58]. Among the various approaches, drop casting is cost-effective, simple, and eco-friendly.

However, only few reports are available for the drop casting of ZnO microstructures at low temperature (80^0C) [59]. No reports are available in the literature for the room temperature drop casting of ZnO nanostructures on the MWCNT surface for HRP immobilization. Keeping all of these interesting facts about MWCNT and ZnO in mind, a novel H_2O_2 biosensor was made in this study using MWCNT/ZnO composite as a matrix and HRP.

2.5 Electrochemistry

Electrochemistry can be defined as the study of production of electricity from energy released during spontaneous chemical reactions and the use of electrical energy to bring about non-spontaneous chemical transformations[60]. This branch of chemistry studies chemical reactions that involve the transfer of electrons between electrodes and reactant molecules in a solution producing electric power[60]. The electrochemical techniques are used for the determination and detection of quite a various range of substances.

For this study a three electrode system is used for the electrochemical study and the cell is monitored by a combination of a computer and a potentiostat/galvanostat[61]. A chemical reaction is brought about by application of excess voltage from an external power and the resultant current flow is measured to obtain characteristics of the analyte of interest.

2.5.1 Voltammetry

In voltammetry a time dependent potential is applied to an electrochemical cell, and the current flowing through the cell is measured as a function of time. Voltammetric methods enable the sensitive and selective measurement of compounds based on their specific electrochemical behavior at the working electrode surface[62]. It makes use of a three electrode system potentiostat that measures current as a function potential. The cell is made up of three electrodes

immersed in a solution containing the analyte and also an excess of a non reactive electrolyte called a supporting analyte. One of the three electrodes is the working electrode, whose potential is varied linearly with time. Its dimensions are kept small to enhance its tendency to become polarized. The second electrode is a reference electrode whose potential remains constant throughout. The third electrode is a counter electrode, which is often a coil of platinum wire that simply conducts electricity from the signal source through the solution to the working electrode [63]. Electrochemical methods are very useful if the selectivity achieved eliminates the need for separation procedures, which simplifies procedures, enables short analysis times and lower cost of analysis by using a relatively cheaper instrument and less consumables[64].

2.5.2 Mass Transfer in Voltammetry

Electron transfer in voltammetry can be influenced by the mass transfer for ions to move towards or away from the electrode. The movement of electron in an electrochemical cell is controlled by mass transport processes and mechanisms involved in the mass transport. There are three types of mass transfer processes to or from an electrode surface[65].

2.5.2.1 Diffusion

It is the movement of a chemical species from a region of high concentration to a region of low concentration under the influence of a concentration gradient.

2.5.2.2 Convection

Convection occurs when a mechanical means is used to carryreactants toward the electrode and to remove products from theelectrode.The most common means of convection is to stir the

solutionusing a stir bar. Other methods include rotating the electrode and incorporating the electrode into a flow cell.

2.5.2.3 Migration

Migration occurs when charged particles in solution are attractedor repelled from an electrode that has a positive or negativesurface charge.Unlike diffusion and convection, migration only affects themass transport of charged particles. There are versatile techniques that can be used in voltammetry and these include cyclic voltammetry, chronoamperometry, impedance spectroscopy, linear scan, square wave voltammetry and differential pulse voltammetry.

2.5.3 Cyclic voltammetry

Cyclic voltammetry (CV) has become an important and widely used electro analytical technique in many areas of chemistry. It is often used to study a variety of redox processes, to determine the stability of reaction products, the presence of intermediates in redox reactions, reaction[66] and electron transfer kinetics, [67] and the reversibility of a reaction. CV can also be used to determine the electron stoichiometry of a system, the diffusion coefficient of an analyte, and the formal reduction potential of an analyte, which can be used as an identification tool. In addition, because concentration is proportional to current in a reversible, Nernstian system, the concentration of an unknown solution can be determined by generating a calibration curve of current vs. concentration.

Cyclic Voltammetry is a technique devoted to the theoretical study of the behavior of redox couples. Cyclic Voltammetry performs a triangular shaped scanning at the working electrode. In this way a redox couple in solution is exposed before to an oxidation and afterwards to a reduction (or vice and versa)[68]. The plot of a cyclic voltammetry consist on a close curve:

reversible redox couples show both as cathodic and anodic peak, while irreversible redox systems show only one peak.

The following relations can be useful to establish the standard potential of a reversible redox couple and the number of electrons involved in the discharge process:

$$E^{O} = \frac{Epa - Epc}{2} \quad (2.7)$$

$$E_{pc} - E_{pa} = \frac{57mV}{n} \quad (2.8)$$

And where E_{pa}= anodic peak potential, in mV and E_{pc}= cathodic peak potential.

2.5.4 Linear sweep voltammetry

Linear sweep voltammetry is a voltammetric method where the current at a working electrode is measured while the potential between the working electrode and a reference electrode is swept linearly in time. Oxidation or reduction of species is registered as a peak or trough in the current signal at the potential at which the species begins to be oxidized or reduced. Linear sweep voltammetry can identify unknown species and determine the concentration of solutions. $E_{1/2}$ can be used to identify the unknown species while the height of the limiting current can determine the concentration. The sensitivity of current changes vs. voltage can be increased by increasing the scan rate. Higher potentials per second result in more oxidation/reduction of a species at the surface of the working electrode [69].

2.5.5 Chronoamperometry

Chronoamperometry is an electrochemical technique in which the potential of the working electrode is stepped and the resulting current from faradaic processes occurring at the electrode (caused by the potential step) is monitored as a function of time. Limited information about the identity of the electrolyzed species can be obtained from the ratio of the peak oxidation current versus the peak reduction current. However, as with all pulsed techniques, chronoamperometry generates high charging currents, which decay exponentially with time as any RC circuit

Chronoamperometryis a very powerful method for the quantitative analysis of a nucleation process. This useful technique leads to obtain the initial information about nucleation and growth mechanism in a studied system. Additionally, the amount of charge for deposition (dissolution) can be determined. Also, this method can be applied for the determination of a nucleation rate constant and an adsorption isotherm. With the chronoamperometry, the current is measured versus time as a response to a(sequence of) potential pulse. The recorded current can be analyzed and its nature can be identified from the variations with time[70].

2.5.6 Electrochemical impedance spectroscopy

EIS is a perturbative characterization of the dynamicsof an electrochemical process.A tool for unraveling complex non-linear processes[71] . Electrochemical impedance is the response of an electrochemical system (cell) to an applied potential. The frequency dependence of this impedance can reveal underlying chemical processes.

It is regarded as a derivative of linear sweep voltammetry or staircase voltammetry, with a series of regular voltage pulses overlaid on the potential linear sweep or stair steps. The current is

measured instantaneously before each potential change, and the current difference is plotted as a function of potential [72]. The Nyquist plots obtained in electrochemical impedance spectroscopy comprise of a straight line and a semi-circle. The diameter of the semicircle corresponds to the charge transfer resistance and diffusion controlled process respectively. The straight line portion represents the Warburg impedance which takes into account the frequency dependence on diffusion transportation to the electrode surface [73].

2.7 Summary

Various types of techniques have been utilized for determination of hydrogen peroxide; however electrochemical sensing is becoming wide spread due to its advantages such as simplicity, fastness, high sensitivity and can obtain perfect results with minimum supervision. The immobilization of an enzyme on a MWCNTs and metal nanoparticles matrix is known to improve electrocatalysis by enhancing the surface area of the electrode and yielding excellent catalytic character unlike bare glassy carbon electrodes. Chemical and physical combination of these nanomaterials can produce very efficient electrochemical sensors. Based on this known attractive properties the research was being pursued following a series of sequential steps which are to follow in the next chapter.

CHAPTER 3

MATERIALS AND METHODS

3.0 Introduction

The purpose of this chapter is to highlight the reagents and the procedures which were used in order to achieve the desired aims and objectives. The activity of the immobilized HRP on zinc oxide/ multiwalled carbon nanotubes modified glassy carbon electrode was characterized using cyclic voltammetry andelectrochemical impedance. The electrocatalytic reduction of hydrogen peroxide was studied using cyclic voltammetry, differential pulse voltammetry (DPV) and linear voltammetry. The catalytic effect of the enzyme was studied using chronoamperometry.

3.1 Reagents and chemicals

All the chemicals that were used in this study were of pure analytical grade. Potassium ferrocyanide ($K_3[Fe(CN)_6]$) and Horseradish peroxidase were obtained from Sigma Aldrich(Johannesburg, South Africa), hydrogen peroxide (H_2O_2),potassium chloride (KCl), zinc acetate dihydrate[$Zn(O_2CCH_3)_2(H_2O)_2$] were from Associated Chemical Enterprises (Harare, Zimbabwe). Hydrochloric acid (HCl), sodium hydroxide (NaOH), potassium di-hydrogen phosphate (KH_2PO_4), di-potassium hydrogen phosphate (K_2HPO_4), acetic acid (CH_3COOH) and ethanol (C_2H_5OH) were from Sky labs (Harare, Zimbabwe). Multiwalled carbon nanotubes (MWCNTs) were obtained at Sigma Aldrich (Johannesburg, South Africa). Distilled water was from Midlands State University Chemical Technology laboratory. A stock solution of potassium ferricyanide was dissolved in 1M KCl in a 500 mL volumetric flask. Masses of about 13.06 g of potassium di-hydrogen phosphate and 17.41 g of di-potassium hydrogen phosphate were weighed and each was dissolved and diluted in 100 mL volumetric flask to the mark. A volume of 30.75 mL K_2HPO_4 and 19.25 mLKH_2PO_4 were placed into a 500 mL volumetric flask then

diluted to the mark to make a phosphate buffer solution at a pH of 7.A stock solution of 1 mM hydrogen peroxide was prepared in a 1000 mL volumetric by adding 58.6µL of 20 VOL and filling to the mark with distilled water and it was used for the preceding experiments.

3.2Equipment

All the electrochemical experimental procedures were carried out using Autolab Potentiostat PGSTAT302F installed a 1.10 version NOVA software employing a convectional three electrode system. The three electrode system constituted of a bare glassy carbon electrode of 3 mm in diameter which was the working electrode, a platinum wire which was working as an auxiliary/counter electrode and Ag/AgCl (3.0 M) which was working as the reference electrode. All the experiments that were conducted in this study were carried out at room temperature conditions 25 °C (Zimbabwe). A digital analytical balance (G and G of model JJ224BC) was used for weighing. As for pH studies of the solutions, they were adjusted by a Thermoscientific Orion Star A211 pH meter.

3.3 Synthesis and characterization of ZnO nanoparticles

The synthesis of zinc oxide nanoparticles was carried out by sol gel process, at 80-90^{0}C. A solution of zinc acetate dihydrate [Zn $(O_2CCH_3)_2(H_2O)_2$] was prepared by dissolving 2.195 g of zinc acetate dihydrate in 100 mL ethanol, and stirred in ambient atmosphere. Potassium hydroxide KOH 1.122g was dissolved in 10 mL distilled water and added to the zinc acetate dihydrate-ethanol solution drop wise under continuous stirring. After a few minutes the solution turned into a jelly form and a milky white solution was obtained, the mixture was then further heated for 3h at 80- 90^{0}C without stirring. The resulting suspension was centrifuged to retrieve

the product, and the mixture was washed with distilled water in an ultrasonic bathwater and then the powder dried at 70^{o} C over night [74].

3.4 Enzyme monitoring

The activity of the enzyme was monitored by means of UV-VIS spectroscopy.0.01 mg of HRP, MWCNT and ZnO were dissolved in DMF. The wavelength was scanned from 300 – 800nm for HRP, MWCNT and HRP/ZnO/MWCNT.

3.5 Electrode modification

Prior to modification the glassy carbon electrode was firstly polished using alumina slurry powder on a Buehler-felt pad. Then it was rinsed in distilled water followed by ultra-sonication in a solution of ethanol and distilled water(1:1). Multiwalled carbon nanotubes were dispersed in dimethylformamide (DMF) (1 mg:1 mL) and then ultra-sonicated for about 30 min. ZnO nanoparticles were dispersed in DMF(1 mg:1 mL) and ultrasonicated for 2 h[4]. The drop dry method was employed for the electrode modification were 5µL of MWCNTs and ZnO nanoparticles composite was drop casted on the electrode and left to dry at room temperature [75].The HRP was immobilized by dropping 2 µL of 10 mg/mL of the protein solution onto the MWCNTs/ZnO nanoparticles modified glassy carbon electrode and dried for about 30 min at room temperature.

3.6 Cyclic voltammetry

3.6.1 Electrochemical behavior of modifiers in 10 mM $K_3[Fe(CN)_6]$

Cyclicvoltammetry and electrochemical impedance was used for theinvestigation of electrochemical behavior of the bare GCE, ZnO/GCE, MWCNT/GCE, ZnO/MWCNT/GCE and

HRP/ZnO/MWCNT/GCE electrodes in potassium ferrocyanide solution at a scan rate of 0.1 V/s from -0.4 to 0.6 V. A volume of about 100 ml of potassium ferricyanide were used for all analysis pertain its use.

3.6.2 Effect of pH

Five different 100 mL volumetric flasks were filled with 1 mM hydrogen peroxide solution. Then each solution was adjusted its pH using 0.1 M HCl solution for acidic pH and 0.1 M NaOH solution for basic pH from pH 4 to 8 at a scan rate of 0.1 V/s at a potential range of -1.2 to 0.6 V on HRP/ZnO/MWCNT/GCE.

3.6.3 Effect of scan rate

The effect of scan rate for HRP /ZnO/MWCNT/GCE in1 mM of hydrogen peroxide was carried out in pH 4 of phosphate solution. The scan rates which were applied were 100mV/s, 125 mV/s, 150 mV/s, 175mV/s, 200mV/s, 225 mV/s, 250 mV/s, 275 mV/sand300 mV/s at a potential range of -1.2 to 0.6 V.

3.6.4 Direct electrochemistry of HRP

The direct electrochemistry of HRP was studied using cyclic voltammetry on bare GCE, ZnO/GCE, MWCNT/GCE, ZnO/MWCNT/GCE and HRP/ZnO/MWCNT/GCE electrodes in 0.1 M phosphate buffer (pH 4) in the absence of hydrogen peroxide at a potential of -0.8 to 0.2 V at a scan rate of $0.1Vs^{-1}$

3.6.5 Electrocatalytic detection of hydrogen peroxide

The electrochemical behavior of 1 mM of hydrogen peroxide solution was studied using cyclic voltammetry on bare GCE, ZnO/GCE, MWCNT/GCE and HRP/ZnO/MWCNT/GCE electrodes in 0.1 M phosphate buffer at pH 4 as the supporting electrolyte at 0.1 V/s from- 0.6 to 0.6 V.

3.6.6 Order of reaction

The order of reaction of HRP/ZnO/MWCNT/GCE was studied using linear scan voltammetry in different concentrations of hydrogen peroxide of 0.5 mM,1 mM, 1.5 mM, 2 mM, 2.5 mM and 3 mM at 0.1 V/s scan rateand potential of 0.6 V to -1.2 V.

3.6.7 Impedemetric behavior of the sensor

The impedemetric behavior of the sensor was studied using EIS in different concentrations of hydrogen peroxide of 0.5 mM, 1 mM, 1.5 mM, 2.0 mM, and 2.5 mM. It was carried out in 0.1M PBS at pH 4

3.6.8 Determination of catalytic coefficient

Chronoamperometry was used in the determination of the catalytic constant, LOD, LOQ. Different concentrations of 1.6 µM, 1.8 µM, 2.1 µM, 2.4 µM and 3 µM were run in 0.1 M PBS pH 4 at a potential of -0.33V.

3.6.9 Stability and reproducibility studies

As for the reproducibility studies of the produced sensor, linear sweep voltammetry technique was employed. The assay reproducibility of the sensor was investigated through 4 repetitive measurements of the 1mM hydrogen peroxide sample in 0.1 M phosphate buffer at pH 4 at a potential of -1.2 to 0.6 V starting from the more positive potential to the more negative one.

The stability of HRP/ ZnO/ MWCNT/GCE electrode biosensor was studied using cyclic voltammetry at regular intervals of 7 days for three weeks in 1mM hydrogen peroxide in 0.1M PBS pH 4.0 at a potential of -1.2 to 0.6V. When not in use, the electrode was washed with distilled water and stored in a refrigerator at 4ºC [34].

CHAPTER 4

RESULTS AND DISCUSSION

4.0 Introduction

The chapter deals with the research findings and authentication of the procedures in the methodology section. Preliminary studies were carried out employing cyclic voltammetry with the BGCE, ZnO/GCE, MWCNT/GCE, ZnO/MWCNT/GCE and HRP/ZnO/MWCNT/BGCE electrodes in 10 mM potassium ferricyanide. Chronoamperometry, linear sweep voltammetry and electrical impedance spectroscopy and were used in the electrochemical studies. Selectivity and reproducibility studies were conducted in authenticating the developed sensor

4.1 Monitoring activity of the enzyme

Fig 4.1 shows the UV-visible absorption spectra of MWCNT, HRP and HRP/ZnO/MWCNT films

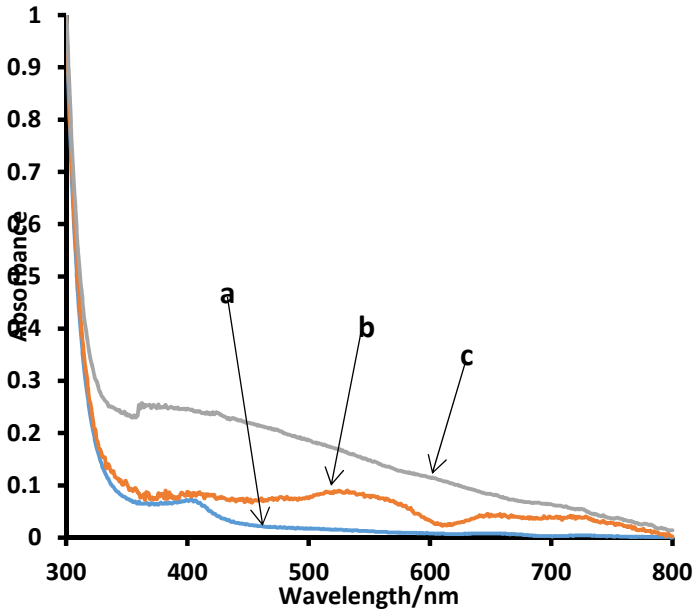

Fig 4.1: UV-vis absorption spectra of MWCNT (a), HRP (b) andHRP/ZnO/MWCNT (c) films.

It is well known that from the exact location and from the shift in position of the soretabsorption band it is possible to confirm the denaturation of heme proteins at the immobilizationmatrix. In this study, UV-visible absorption spectroscopy was used as an effective tool to confirmwhether the HRP retains its native structure at the ZnO/MWCNT matrix.A characteristic absorptionbands were observed in the absorption spectra of MWCNT at 400nm. On the other hand, the heme bands of HRP casted film and HRP in buffer will beobserved at 404 nm and 403 nm, respectively [59]. In the present study, the Soret band of HRP was observed at 407nm and HRP/ZnO/MWCNTcasted film was observed at 390 nm which is close to the heme bands ofHRP reported in the literature. The above discussed UV-visible absorption spectra results reveal thatHRP retains its native structure at the ZnO/MWCNT matrix. Thus the ZnO/MWCNT matrixprovides good biocompatibility for the immobilized HRP.

4.2 Electrochemical behavior of modified electrode in redox probe

The electrochemical properties of bare GCE (*curve a*), ZnO/GCE (*curve b*), MWCNT/GCE (*curve c*), ZnO/MWCNT/GCE (*curve d*) and HRP/ZnO/MWCNT/GCE *(curve e)* were characterized by CV in 10 mM $K_3[Fe(CN)_6]$ solution containing 0.1 M K Cl at 0.1 V/s (fig 4.2)

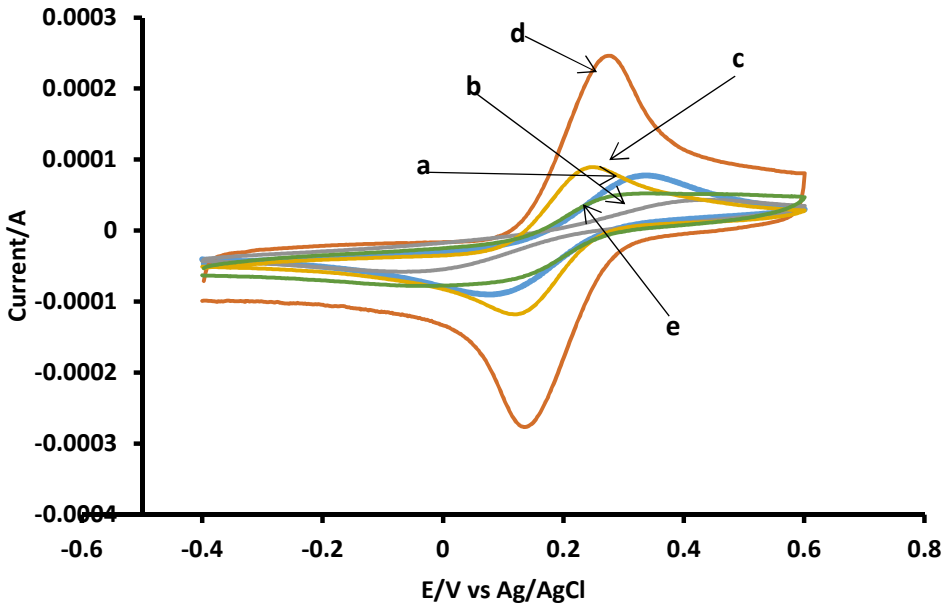

Fig 4.2: Voltammograms for (a) GCE, (b) ZnO/GCE, (c) MWCNT/GCE, (d)ZnO/MWCNT/GCE and (e) HR/ZnO/MWCNT/GCE in 10 mM potassium ferricyanide solution at 0.1 V/s at a potential of -0.4 to 0.6 V

All the electrodes were scanned in 10 mM $K_3[Fe(CN)_6]$ in KCl. The outcome voltammograms are illustrated on Fig 4.2.The different electrodes gave different signals of peak current when they were analyzed in the following descending order ZnO/MWCNT/GCE > MWCNT/GCE > GCE >HRP/ZnO/MWNT/GCE > ZnO/GCE. It can be seen in Fig. 4.2 (curve a-e) that a pair of peaks corresponding to the redox reaction of ferricyanide were observed. The peak-to-peak potential separation is a good measure of the electron transfer ability of the electrode with lower

values showing good electron transfer ability [76], following the order: ZnO/MWCNT/GCE (116mV), MWCNT/GCE (98mV), GCE (96.5mV), HRP/ZnO/MWCNT/GCE (223mV) and ZnO (480 mV). It can be seen that the modification of the GCE with ZnO results in a reduction in anodic peak current of the $[Fe(CN)_6]^{3-/4-}$ (I_{pa}: 5.2×10^{-6} A) compared with the GCE (I_{pa}: 69×10^{-6}A). Compared with ZnO/GCE, the anodic peak current of $[Fe(CN)_6]^{3-/4-}$ ($I_{pa:}236 \times 10^{-6}$A) on MWCNT/GCE further increased. However, the HRP/ZnO/MWCNT/GCE gave an anodic peak current $[Fe(CN)_6]^{3-/4-}$ of (I_{pa}: 39.9×10^{-6}A). This might be attributed to ZnO, an inhibitor hence providing a good immobilization matrix for the enzyme. The obtained results suggested that the HRP/ZnO/MWCNT was successfully adsorbed.

HRP/ZnO/MWCNT/GCE showed the lowest electron-transfer kinetics forming well defined redox peaks with low peak currents and hence was found to be the best electrode. The low peak current potentials exhibited by HRP/ZnO/MWCNT/GCE might have been due to the immobilization of the enzyme. Therefore after the new sensor exhibited better electron transfer properties than the others it was applied for further studies.

4.3 Surface area determination

Scan rate studies for the bare GCE and all modified were done in 5 mM potassium ferricyanide solution by applying the Randles Sevcik equation given on equation 4.1.

$$I_p = (2.69 \times 10^5) n^{3/2} A D^{1/2} V^{1/2} C \qquad (4.1)$$

Where I_p is the peak current, n is equal to the number of electrons transferred to the surface of the electrode which is obtained from equation 4.2.

$$Fe(CN)_6^{3-} + e^- \rightarrow Fe(CN)_6^{4-} \qquad (4.2)$$

Therefore n is equivalent to 1, D gives the diffusion coefficient of the analyte in solution 7.6 x 10^{-6} cm^2/s and C is the concentration of the solution in mol/cm^3. A is the surface area and v scan rate in volts per second. The surface area for the electrode modifiers were obtained as follows ZnO/GCE was 0.030 cm^2, GCE was 0.0712 cm^2, MWCNT/GCE was 0.083 cm^2 ZnO/MWCNT/GCE 0.092cm^2 and 0.123cm^2 for HRP/ZnO/MWCNT/GCE. The surface of the newly modified electrode ZnO/MWCNT/GCE was as twice as that of the bare electrode meaning that the electron catalytic activity of the electrode was enhanced.

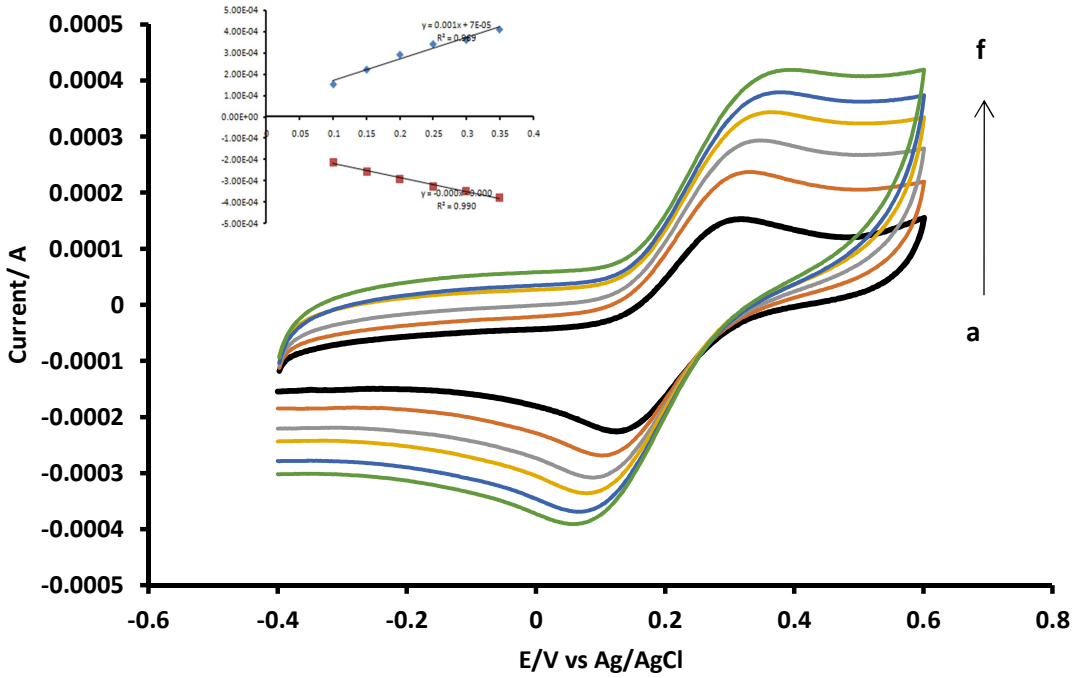

Fig 4.3: Effect of scan rate on peak potentials and peak currents (a) 100 mV/s, (b) 150 mV/s, (c) 200 mV/s, (d) 250 mV/s, (e) 300mV/s, (f) 350 mV/s, on HRP/ZnO/MWCNT/GCE. *Inset* shows peak current against scan rate

4.4 Electrochemical impedance spectroscopy

The electrochemical behavior of the five electrodes was further investigated using the electrochemical impedance spectroscopy (EIS) in 10.0 mM of potassium ferricyanide solution. The Nyquist plots in Figure 4.4 of the electrodes comprised of semicircles and straight line portions. The semicircle part at higher frequencies represents the electron transfer limited process and its diameter is equated to the electron transfer resistance showing the electron transfer kinetics of the redox probe on the interface of the electrode [73]. The representative circuit for the Nyquist plots shown by insert in Figure 4.4 where, RS, CPE, RCT and W represent solution resistance, a constant phase element, the charge transfer resistance and the Warburg impedance respectively[77]. Compared with other electrodes, an enlarged semicircle is found in the Nyquist plot of HRP/GCE (*curve f*) suggesting that HRP acted as an insulating layer and barrier. It also reveals sluggish electron transfer. On the other hand, ZnO/GCE too exhibits an enlarged semicircle than bare/GCE, which also reveals a sluggish electron transfer.The GCE (*curve a*) displays a small semi-circle indicating a low resistance in transfer of electrons. The MWCNT/GCE (*curve b*) showed less resistance and the ZnO/MWCNT/GCE (*curve d*) showed a plot which was almost a straight line indicating a very high electron transfer.

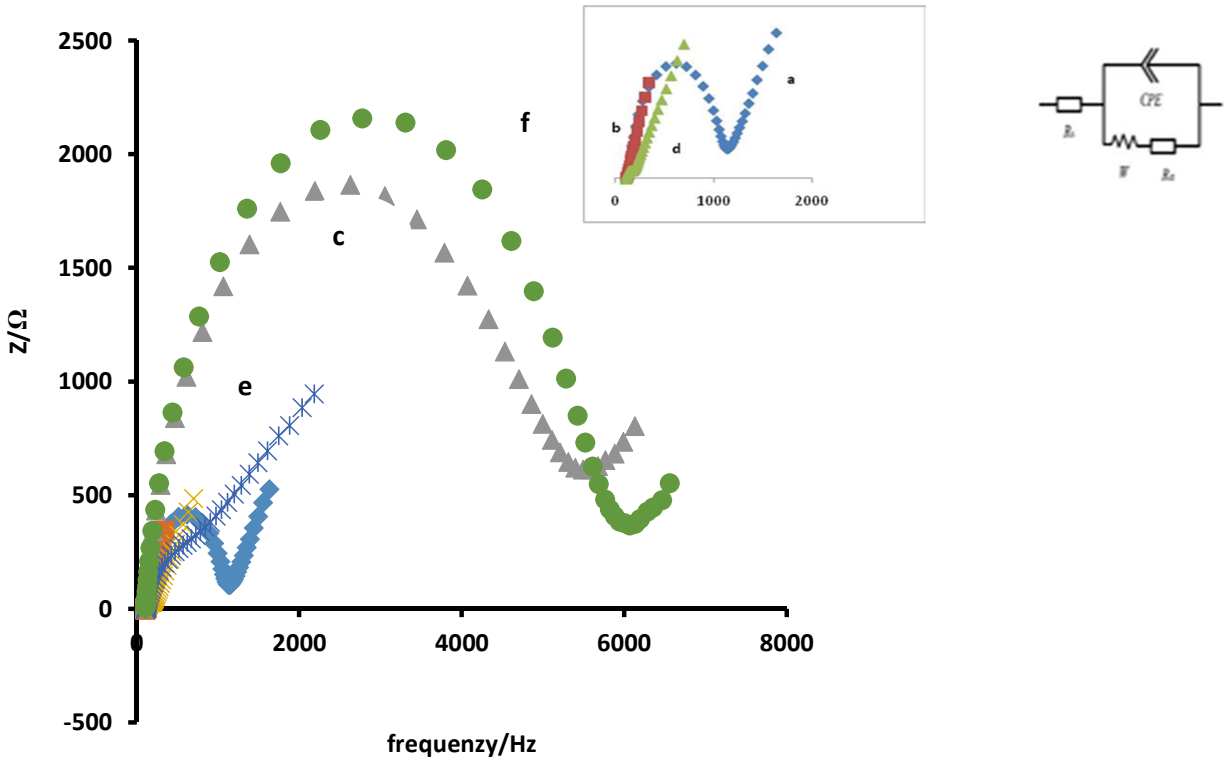

Fig 4.4: Electrochemical impedance graphs for (a) GCE, (b) MWCNT/GCE, (c) ZnO/GCE, (d) ZnO/MWCNT/GCE,(e) HRP/ZnO/MWCNT/GCE and (f) HRP: *Inset* shows the equivalent circuit used for data fitting

4.5 pH studies

The redox behavior of most biomolecules especially enzymes is affected by the pH of supporting electrolyte [78]. The dissociation or reactivity of biological molecules vary from molecule to molecule some react easily at low and some at high pH which is due the effect of different functional groups within the molecule structure. The presence of electron donating groups tend to cause an increase in acidity as they decrease polarity of a most biomolecules [79].

The effect of pH on HRP/ZnO/MWCNT/GCE was examined and the resulting voltammograms were obtained as shown on fig 4.5. As the pH increased from pH 4 to pH 8 the peak current decreased. The maximum peak response was obtained at pH 4.

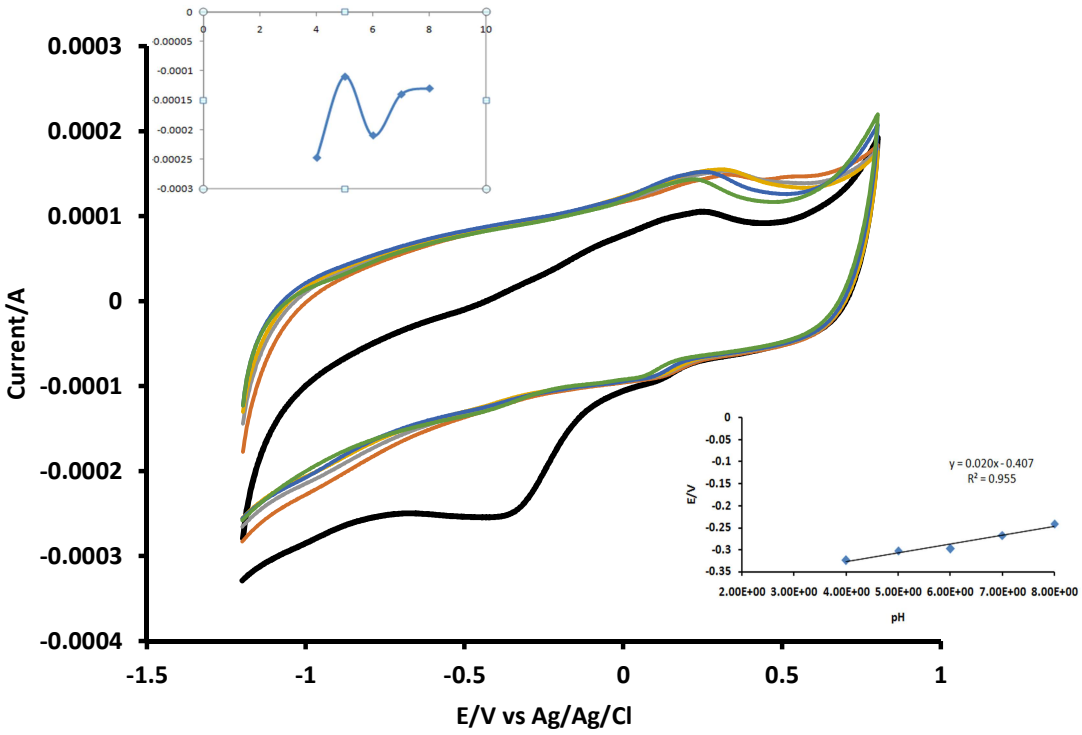

Fig 4.5: Cyclic voltammograms of 1 mM hydrogen peroxide solution at different pH values of 0.1 M PBS:*Inset* shows plot of current against pH, E vs pH

4.6 Direct electrochemistry of HRP

Fig 4.6shows the cyclic voltammograms of different modified GCEs obtained at a scan rate of 0.1 Vs^{-1} in 0.1 M PBS (pH 4.0).

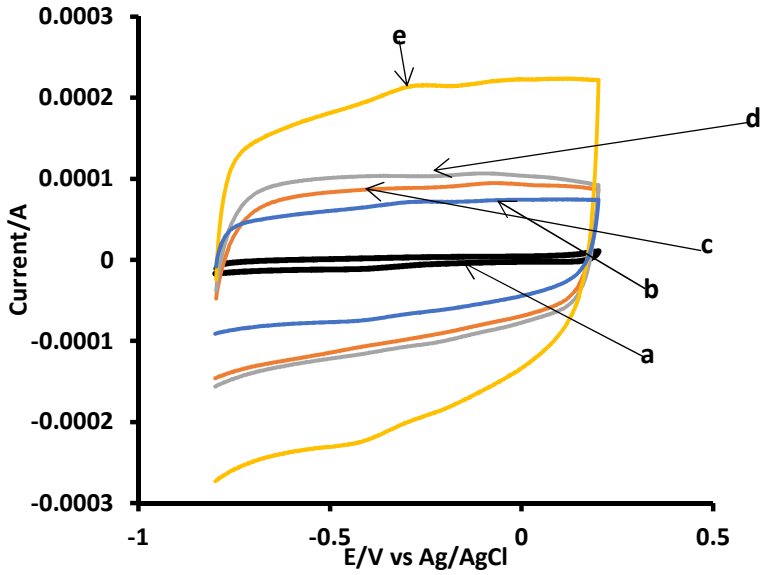

Fig 4.6: (A) Cyclic voltammograms obtained at bare GCE (a), MWCNT/GCE (b), ZnO/GCE (c), ZnO/MWCNT/GCE (d), and HRP/ZnO/MWCNTGCE (e) electrodes in deoxygenated 0.1M PBS (pH 4.0) at a scan rate of 0.1 V s^{-1}

Cyclic voltammograms were recorded in the potential range of -0.8 to 0.2V. Bare GCE does not show any characteristic peaks in this potential window (curve a). Likewise, MWCNT (curve b) and ZnO/MWCNT (curve c) modified electrodes also do not show any characteristic peaks; however, the background current of the latter is higher, clearly indicating that ZnO/MWCNT has higher active electrode area than that of MWCNT. At the HRP/ZnO/MWCNT modified electrode, pair of well-defined redox peaks appears at -0.33 and -0.41V, indicating that the direct electron transfer of HRP has occurred and it has been augmented in the presence of both MWCNT and ZnO.

The peak potential separation (ΔEp) was approximately 136 mV, which was smaller than that of other HRP immobilized carbon nanotubes composite[11]. Such a small peak potential separation value revealed a fast and irreversible electron transfer process. This result indicates that the synergetic effect of ZnO and MWCNT played a more important role in facilitating the direct electron transfer of HRP than bare ZnO/GCE, MWCNT/GCE modified GCEs. The fast electron transfer of HRP can be attributed to the good biocompatibility, large surface area, and high electronic communication capability of MWCNT/ZnO composite.

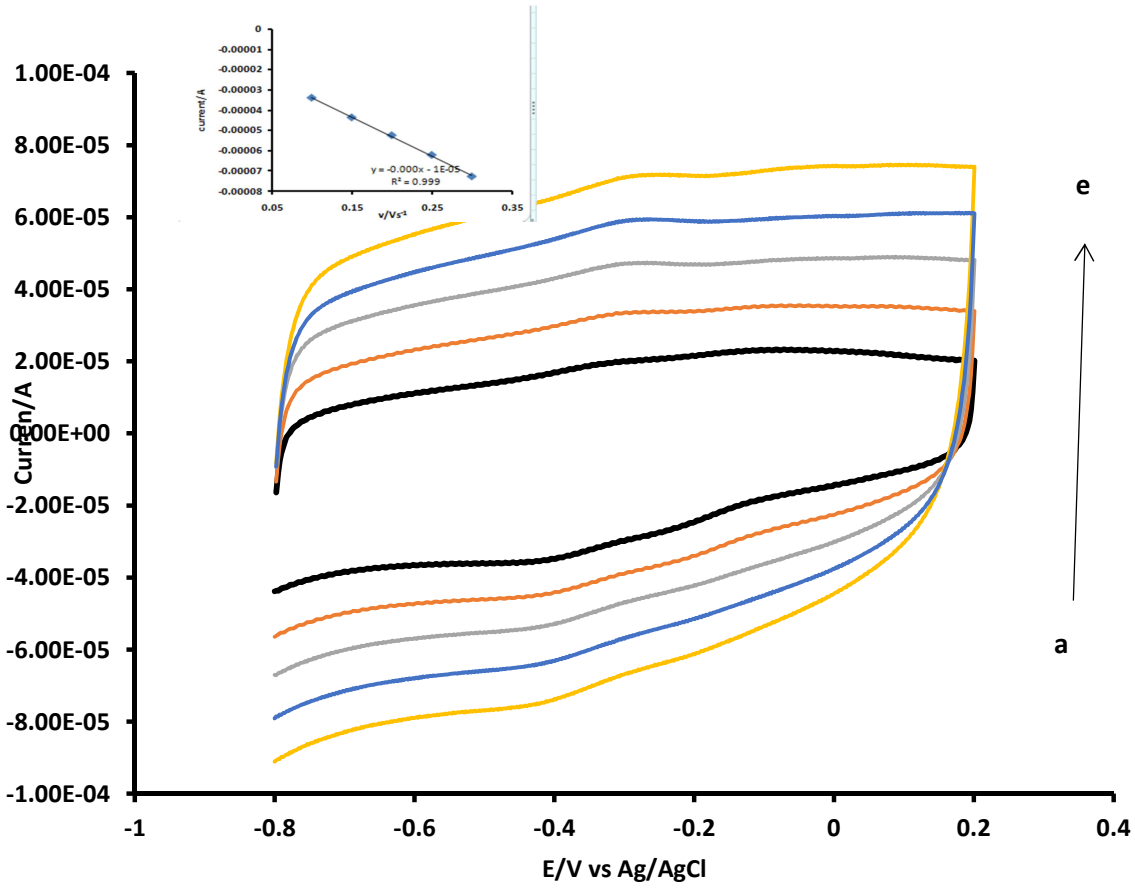

Fig 4.7: Cyclic voltammograms recorded at HRP/ZnO/MWCNT/GCE in deoxygenated 0.1M PBS (pH 4.0) at different scan rates(a) 100 mV/s, (b) 150 mV/s, (c) 200 mV/s, (d) 250 mV/s, (e) 300mV/s.

4.7 Electrocatalytic detection of hydrogen peroxide

As shown in Fig 4.8 peak current increased according to the following sequence of electrode modification on the electrode GCE < ZnO/GCE< MWCNT/GCE< ZnO/MWCNT/GCE< HRP/ZnO/MWCNT/GCE. In the presence of the GCE the reduction of the hydrogen peroxide exhibited high peak potential value while the HRP/ ZnO/MWCNT/GCE showed to have the lowest potential due to synergistic effect of the combination of the nano structures. The inset 4.8 shows the relationship between peak currents and all the probes used in the study.

According to the results it shows that there was a decrease in peak potential from GCE which had the highest to HRP/ZnO/MWCNT/GCE which had the lowest peak potential. The new probe reduced the over potentials which were being exhibited by the bare electrode proving that it was an improved sensor and that it had better electrocatalytic properties.

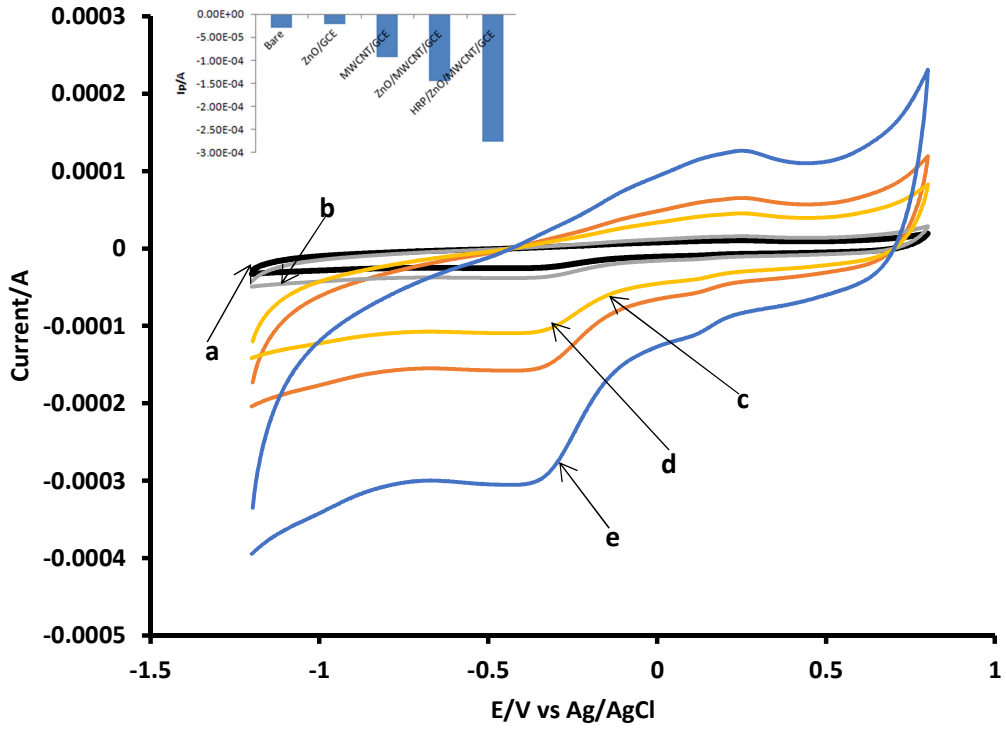

Fig 4.8: The different cyclic voltammograms of hydrogen peroxide on GCE (*curve a*), ZnO/GCE *(curve b)*, MWCNT/GCE (*curve c*), ZnO/MWCNT/GCE (*curve d*) and HRP/ZnO/MWCNT/GCE *(curve e)* in a 0.1 M PBS (pH 4.0) at a scan rate of 0.1 V/s.

4.8 Different scan rate studies at HRP/ZnO/MWCNT composite modified electrode

Fig 4.9 shows the cyclic voltammograms obtained at HRP/ZnO/MWCNT composite film modified GCE in deoxygenated PBS at different scan rates

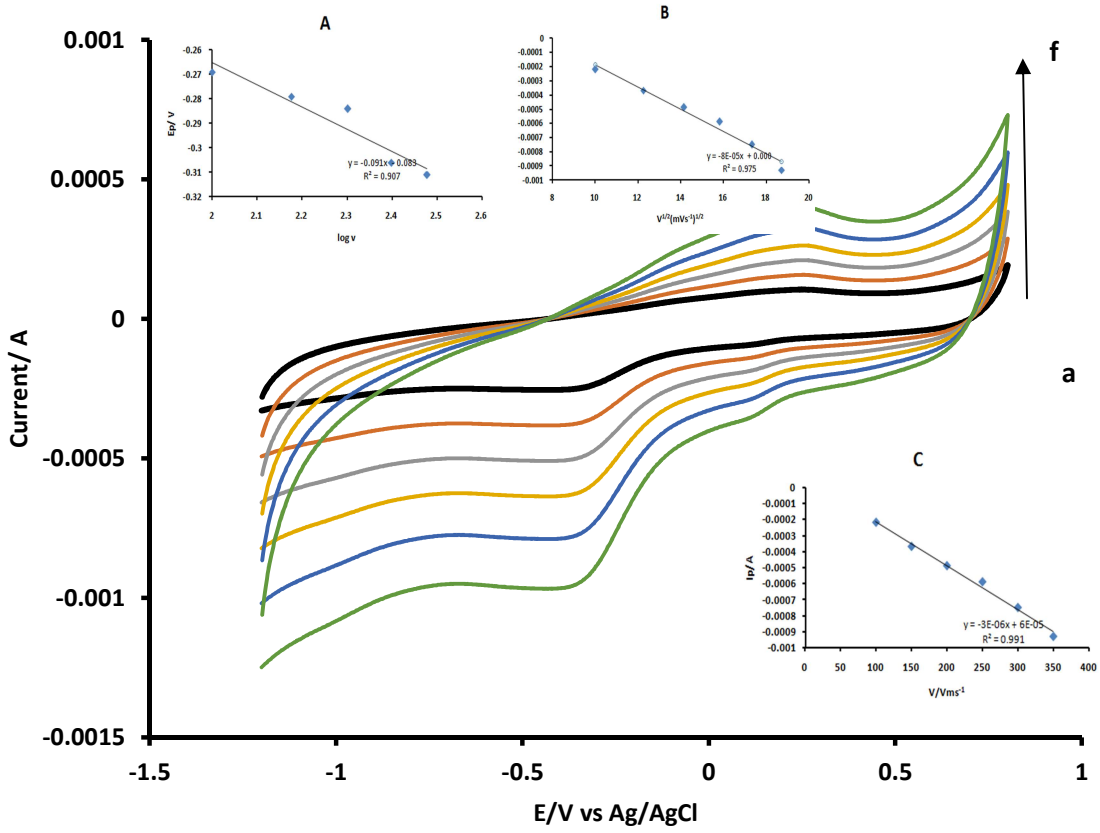

Fig 4.9: Cyclic voltammograms of the detection of hydrogen peroxide at different scan rates(a) 100 mV/s, (b) 150 mV/s, (c) 200 mV/s, (d) 250 mV/s, (e) 300mV/s, (f) 350 mV/s on HRP/ZnO/MWCNT/GCE. *Insets* show plot of reduction peak potential vs. log v and plot of reduction Ip vs.$v^{1/2}$ (scan rate) in 1mM hydrogen peroxide using HRP/ZnO/MWCNT/GCE: 0.1M PBS pH 4.0

On increasing the scan rates, the redox peak currents and peak separation increased linearly. Meanwhile, the cathodic peak potentials showed a small shift and the peak-to-peak separation also increased. The cathodic peak currents increased linearly with scan rates from 100 to 350 mV/s(Fig 4.9 B inset). In addition, the cathodic peak potentials shifted toward the negative direction, and it was clear that HRP absorbed onto the ZnO/MWCNT composite matrix underwent a surface-controlled, quasi-reversible process. The electron transfer rate constant (ks) for HRP at HRP/ZnO/MWCNT composite film modified GCE was calculated using equation 4.3.

$$LogKs = \propto \log(1-\propto) + (1-\propto) log \propto - \log\left(\frac{RT}{nFv}\right) - \frac{\propto(1-\propto)nF\Delta Ep}{2.3RT} \quad (4.3)$$

where R is the gas constant (8.314 J mol^{-1} K^{-1}), T is the room temperature (298.15 K), and ΔEp is the peak separation of the redox couple. Here, the α value was assumed as 0.5 and the number of electrons transferred was considered as 1. The ks value at MWCNT/ZnO/HRP composite film was calculated to be 0.19 s^{-1}, and it was higher than the values of HRP and Hb immobilized at, carbon nanotubes (0.062 s^{-1}) [80]. These results demonstrated that MWCNT/ZnO matrices efficiently facilitated the electron transfer process between HRP and the electrode surface.

The change in the scan rate is accompanied by a shift in peak potential which is suggestive of a reversible reaction during oxidation or reduction of hydrogen peroxide on the modified electrode surface (Fig 4.9). The relationship between reduction peak potential and log of scan rate, Fig 4.9A, for a reversible diffusion-controlled process is given by

$$E_p = \frac{b}{2logv + constant} \quad (4.4)$$

where v is the scan rate and b is the Tafel slope.The Tafel was found to be 182 mV/decade.

The plot in fig 4.9 C confirms that the catalytic detection of hydrogen peroxide is diffusion controlled.

4.9 Impedimetric biosensor for H_2O_2 determination using HRP/ZnO/MWCNT film modified electrode

In order to develop an impedimetric biosensor, EIS measurements were performed at the HRP/ZnO/MWCNT film in the presence of various H_2O_2 concentrations.

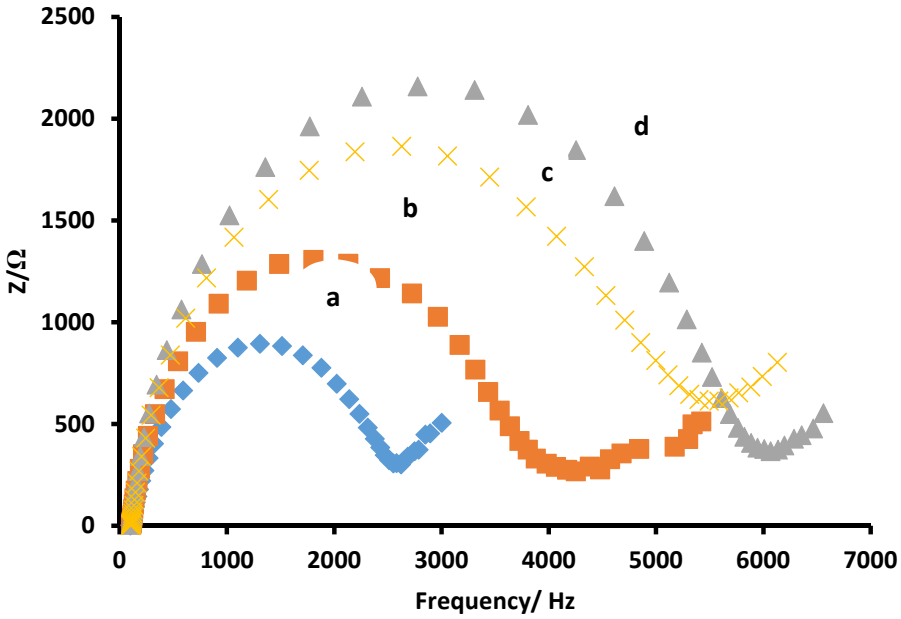

Fig 4.10: Impedimetric response obtained at HRP/ZnO/MWCNT/GCE in presence of various H_2O_2 concentrations i.e. from 1.0 mM (a) - 2.5 mM (d) in 0.1MPBS pH 4.0.

The obtained Nyquist plots are shown in Fig4.10. In the Nyquist plots, the semicircles from inner to outer are the impedimetric responses obtained at HRP/ZnO/MWCNT/GCE for 1 mM – 2.5 mM H_2O_2 (a-d) concentration additions. It is clear that the semicircle diameter increased with

increase in H_2O_2 concentration additions. Similar results have been reported at other impedimetric sensors developed for glutamate , melamine and Uranyl ion (UO^{22}) determinations [81], in which they observed an increase in semicircle diameter while increasing melamine, glutamate and UO^{22+} concentrations, respectively. In the present study, the reason for the augmentation in semicircle diameter with increase in H_2O_2 concentrations could be attributed to the insulation layer formed by the adsorbed H_2O_2 at modified electrode surface which inhibits the charge transfer for the redox probe. However, only limited reports are available for H_2O_2impedimetric biosensors. The good impedimetric H_2O_2 detection results achieved at the HRP/ZnO/MWCNT film in this study could be attributed to the excellent biocompatibility of MWCNT film, good conductivity of ZnO, and the good affinity of the composite film towards H_2O_2.

4.10Linear sweep voltammetry

Linear sweep voltammetry (LSV) was done to show adsorption behavior of HRP/ZnO/MWCNT/GCE and explain the high Tafel slope observed. Fig 12(A) shows LSV plots obtained after keeping the electrode in a stirred solution for 20 minutes (to allow for adsorption). Applying the Langmuir adsorption theory (Eq. 4.5 [76]) a plot of the ratio of hydrogen peroxide concentration to catalytic current against concentration of hydrogen peroxide gave a linear plot which is indicative of adsorption further consolidating the observed high Tafel slopes.

$$\frac{[H2O2]}{Icat} = \frac{I}{\beta Imax} + \frac{[H2O2]}{Imax} \qquad (4.5)$$

where β is the adsorption equilibrium constant, I_{max} is the maximum current and I_{cat} is the catalytic current. From the slope and the intercept of Fig 4.10(inset), the adsorption equilibrium constant b was established to be 1.578×10^3 M^{-1}. Using equation 4.6 which relates Gibbs free energy change due to adsorption (ΔG^o) to the adsorption equilibrium constant b, ΔG^o was found to be 18.45 k J mol^{-1}. This value is comparable to those reported elsewhere for high Tafel slopes [76].

$$\Delta G^o = RT\ln\beta \qquad (4.6)$$

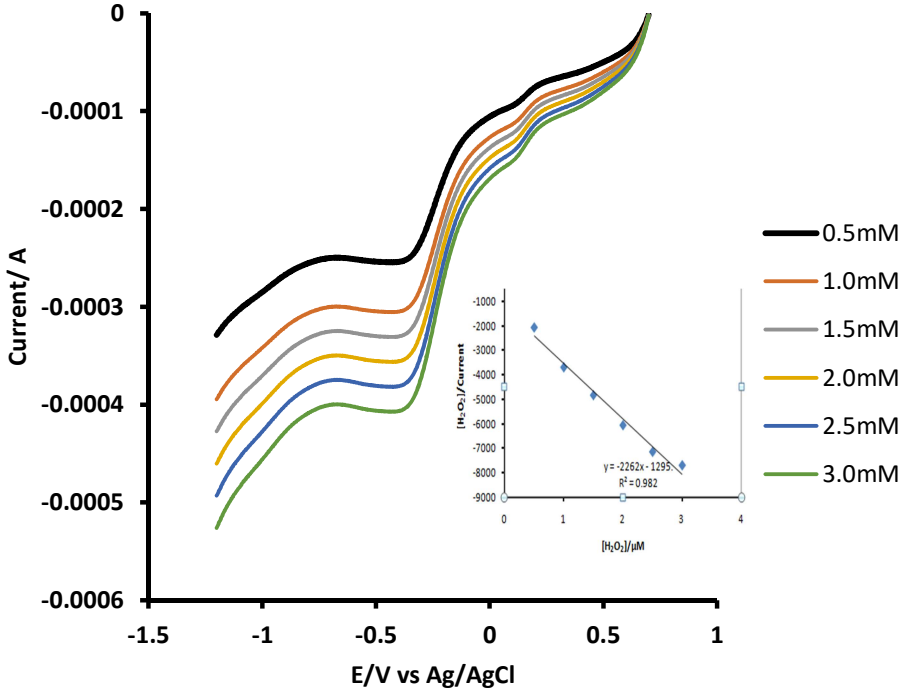

Fig 4.11: Linear sweep voltammograms and *inset* Langmuir adsorption isotherm plot for HRP/ZnO/MWCNT/GCE in 1μM hydrogen peroxide: (pH 4.0) 0.1M PBS buffer. Reduction currents employed.

4.11 Chronoamperometry studies

Chronoamperometry was used to determine the nanoprobe sensitivity, rate constants, diffusion coefficient and the detection limits. Within the first 5 s (on average), the catalytic current is dominated by electro reduction of hydrogen peroxide in this work (Fig. 4.12A). According to literature, the rate constant can be evaluated using

$$\frac{Icat}{Ibuffer} = \frac{\gamma^{1/2}(\pi^{1/2}\,\mathrm{erf}(\gamma^{1/2})+e^{-\gamma}}{\gamma^{1/2}} \quad (4.7)$$

Where I_{cat} and I_{buf} are the currents on the modified GCE in the presence and absence of hydrogen peroxide, respectively, and $\gamma = kC_o t$ (C_o is the bulk concentration of hydrogen peroxide) and erf is the error function.

In cases where g exceeds 2, the error function is almost equal to 1 and the above equation can be reduced to

$$\frac{Icat}{Ibuffer} = \gamma^{1/2}\pi^{1/2} = \gamma^{1/2}(kCot) \quad (4.8)$$

where k is the catalytic rate constant, Co is the bulk concentration of hydrogen peroxide and t is the time elapsed in seconds. Fig 4.12B shows the plots of (I_{cat}/I_{buf}) versus $t^{1/2}$ for hydrogen peroxide oxidation. The slopes of the plots of (I_{cat}/I_{buf}) versus $C_0^{1/2}$ were used to calculate the rate constant according to Equation 4.9. The slope is equal to πk where k is the rate constant. For HRP/ZnO/MWCNT/GCE

$y=3.15x - 3.350$; $r^2= 0.918$ (4.9)

The rate constant was found to be 1×10^3 $M^{-1}s^{-1}$ which compares very well with those reported by Ganesan and Ramaraj (2009)[16] who obtained catalytic rate constants ranging from 8×10^1 $M^{-1}s^{-1}$ to 1.29×10^3 on HRP modified electrodes.

The diffusion constant was deduced from the plot of concentration vs slope (Fig 4.13 D) and was found to be 0.835 cm^2/s.

Fig 12 (A)

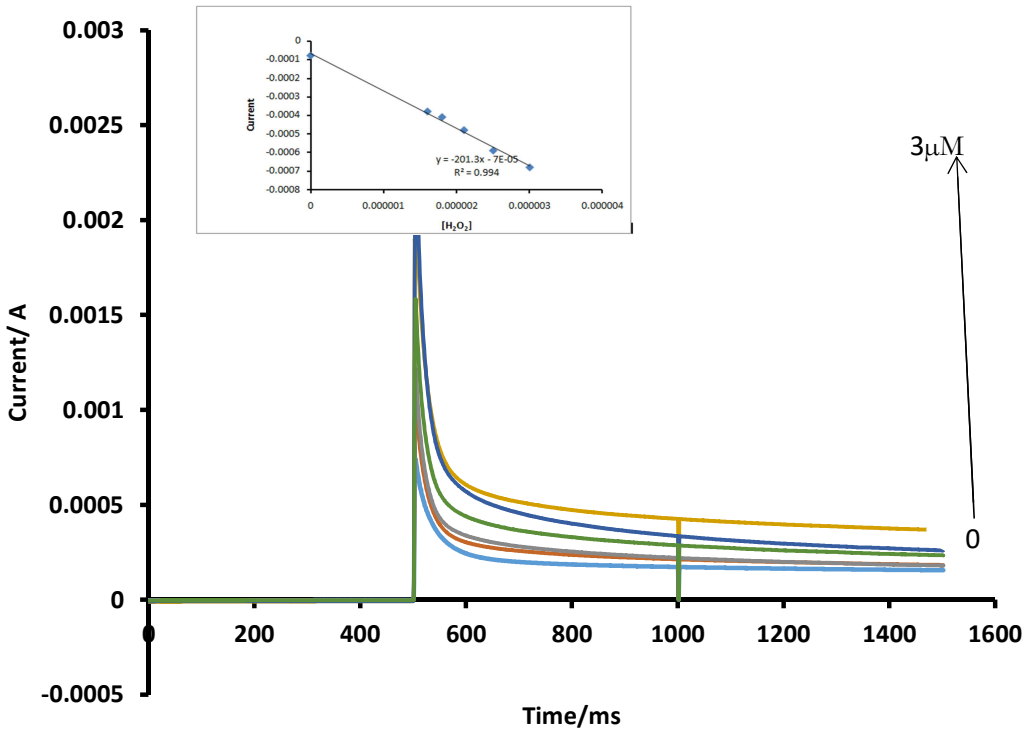

Fig 12 (B)

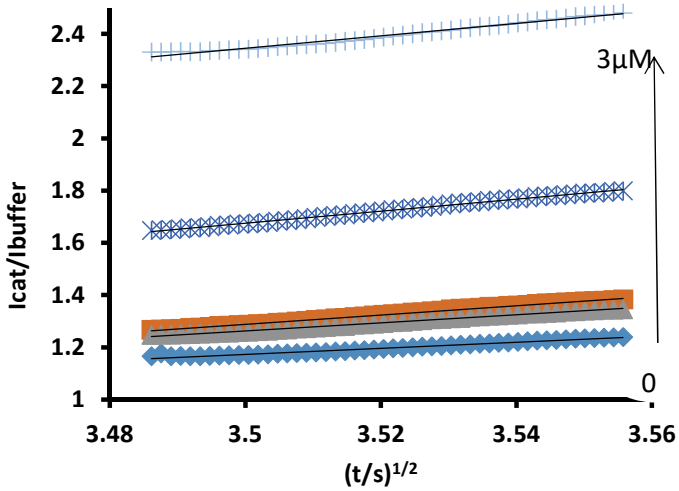

Fig 12 (C)

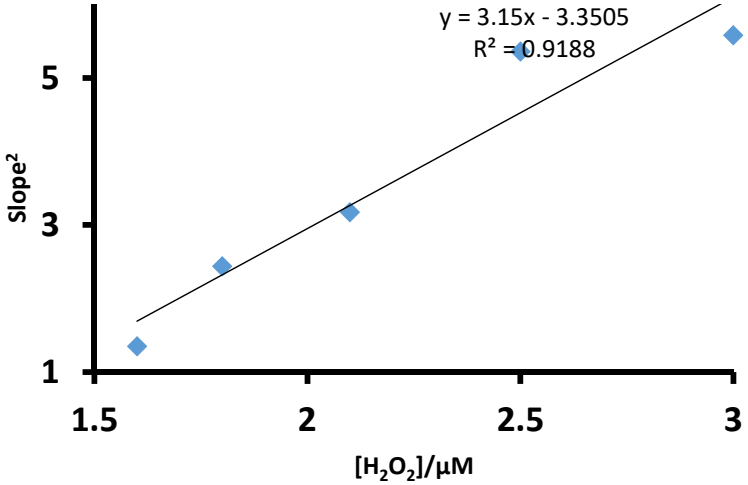

Fig 12 (D)

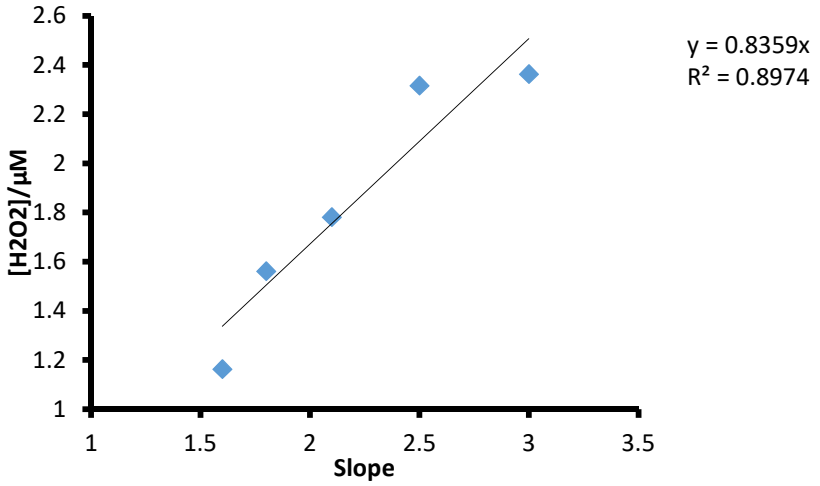

Fig 4.12: (A) Chronoamperograms, (*Inset* t = dependence of concentration on current), (B) Plots of I_{cat}/I_{buf} versus $t^{1/2}$ (1.60 µM, 1.80 µM, 2.10µM, 2.50 µM, and 3.00 µM, 0.22 mM, at- 0.33 V.) determined using chronoamperometry for HRP/ZnO/MWCNT/GCE

4.12 Limit of detection

Limits of detection (LOD) values were calculated using the 3s notation, and using the insert in Fig. 4.12(A) HRP/ZnO/MWCNT/GCE showed an LOD of 3.48 x 10^{-7}M which is in the range of literature values [8].

$$\text{LOD} = \frac{3S}{m} \qquad (4.10)$$

Where S is the standard deviation of the blank and m is slope of the calibration curve.

4.13.1Reproducibility

The newly developed sensor showed a slight decrease in the peak current after washing the electrode three different times with ethanol and water solution ratio one as to one. A relative standard deviation of 3.25 % was found and this indicated good repeatability.

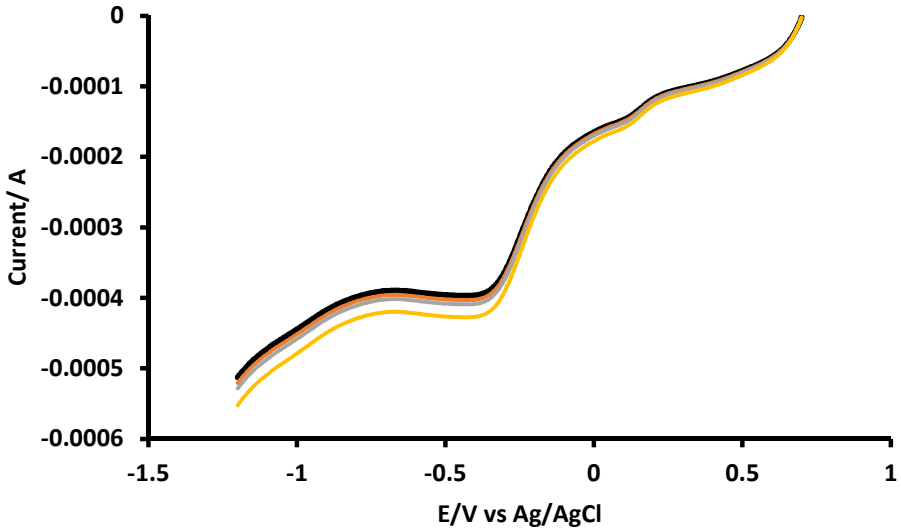

Fig 4.13: Linear sweep voltammograms for four repetitions in 1 mM solution at HRP/ZnO/MWCNT/GCE electrode at a scan rate of 100 mV/s and a potential range of -1.2 V to 0.6 V.

4.13.2 Stability

The stability of HRP/ ZnO/ MWCNT/GCE electrode biosensor was checked by carrying out experiments at the regular interval of a week and it has been found that HRP/ ZnO/ MWCNT/GCE based biosensor retains its 95% activity after 21 days. The loss in the activity of biosensor might be due to the denaturation of Horseradish peroxidase and to the poor adhesion of ZnO/MWCNT on the carbon paste electrode [34]

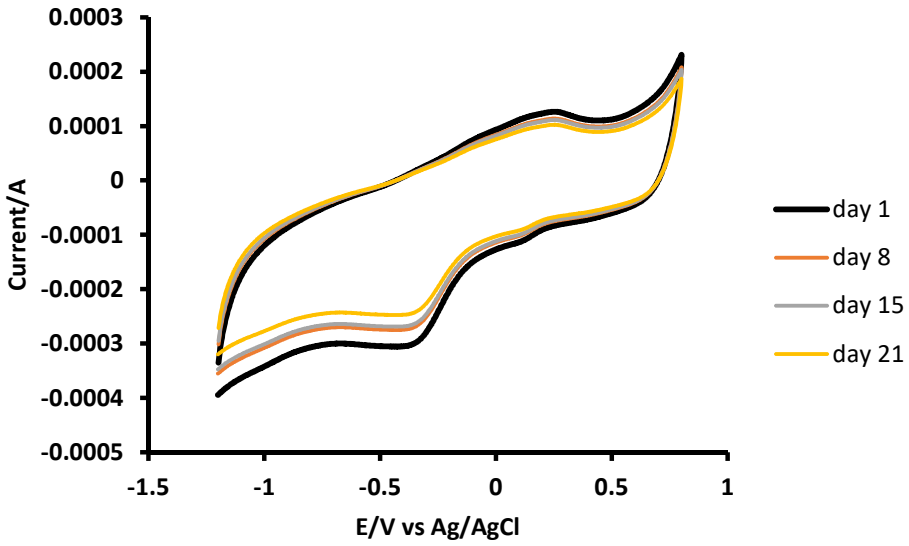

Fig 4.14: Cyclic voltammograms of the detection of 1 mM hydrogen peroxide at regular intervals for 21 days

.

CHAPTER 5

CONCLUSION AND RECOMMENDATION

5.0 Conclusion

A new biosensor based on the immobilization of HRP on a ZnO-MWCNT composite modified glassy carbon electrode was successfully prepared, characterized and utilized for the electrochemical determination of hydrogen peroxide. The immobilized enzyme on the ZnO-MWCNT composite showed enhanced sensitivity and this was achieved due to its ability to amplify signals and increase the electroactive surface area of the electrode. The biosensor, HRP/ZnO/MWCNT/GCE revealed good reproducibility, sensitivity and stability towards hydrogen peroxide andthe method showed to be simple and less time consuming for determination of hydrogen peroxide. The detection limit was3.48×10^{-7}M. The catalytic rate constant of the developed biosensor was found to be 1×10^{3} $M^{-1}s^{-1}$

5.1 Recommendations

Further studies can still be done in order to enhance the performance of this newly developed biosensor. This can be achieved by employing new methods which effectively bind ZnO onto MWCNT surface such as cross linking and also better methods can be identified for binding HRP onto theZnO-MWCNT matrix onto electrode surface which includes the use of binders such as Nafion film.

REFERENCES

[1] Petri BG, Watts RJ, Teel AL, Huling SG, Brown RA. Fundamentals Of Isco Using Hydrogen Peroxide. 2011.

[2] Salimi A, Noorbakhash A, Karonian FS. Carbon Based Enzymeless Hydrogen Peroxide Sensor and Further Applications. Int J Electrochem Sci 2006;1:435–46. 2016.

[3] Botero-Cadavid JF, Brolo AG, Wild P, Djilali N. Detection of hydrogen peroxide using an optical fiber-based sensing probe. Sensors Actuators, B Chem 2013;185:166–73. doi:10.1016/j.snb.2013.04.068.

[4] Moyo M, Okonkwo JO. Horseradish peroxidase biosensor based on maize tassel-MWCNTs composite for cadmium detection. Sensors Actuators, B Chem 2014;193:515–21. doi:10.1016/j.snb.2013.11.086.

[5] Rahman MM, Ahammad AJS, Jin JH, Ahn SJ, Lee JJ. A comprehensive review of glucose biosensors based on nanostructured metal-oxides. Sensors 2010;10:4855–86. doi:10.3390/s100504855.

[6] Ramachandran R, Chen SM, Gnana Kumar GP, Gajendran P, Xavier A, Biruntha Devi N. High electroactive electrode catalysts and highly sensitive electro analytical techniques for hydrogen peroxide detection. Int J Electrochem Sci 2016;11:1247–70.

[7] M. AK, Jung S, Ji T. Protein Biosensors Based on Polymer Nanowires, Carbon Nanotubes and Zinc Oxide Nanorods. Sensors 2011;11:5087–111. doi:10.3390/s110505087.

[8] Ahammad AJS. Hydrogen Peroxide Biosensors Based on Horseradish Peroxidase and

Hemoglobin 2013:1–11. doi:10.4172/2155-6210.S9-001.

[9] Huang S, Qu Y, Li R, Shen J, Zhu L. Biosensor based on horseradish peroxidase modified carbon nanotubes for determination of 2,4-dichlorophenol. Microchim Acta 2008;162:261–8. doi:10.1007/s00604-007-0872-2.

[10] Neal C. Fabrication and Investigation of an enzyme-free , Nanoparticle-based Biosensor for Hydrogen Peroxide determination. "Applied Catal B, Environ 2014;148-149:22–8. doi:10.1016/j.apcatb.2013.10.044.

[11] Palanisamy S, Cheemalapati S, Chen SM. Enzymatic glucose biosensor based on multiwalled carbon nanotubes-zinc oxide composite. Int J Electrochem Sci 2012;7:8394–407.

[12] Scandurra G, Arena A, Ciofi C, Saitta G. Electrical Characterization and Hydrogen Peroxide Sensing Properties of Gold/Nafion:Polypyrrole/MWCNTs Electrochemical Devices 2013:3878–88. doi:10.3390/s130303878.

[13] Walter EC, Zach MP, Favier F, Murray BJ, Inazu K, Hemminger JC, et al. Metal nanowire arrays by electrodeposition. ChemPhysChem 2003;4:131–8. doi:10.1002/cphc.200390022.

[14] Aldeen E. The Electrochemical Oxidation Of Hydrogen Peroxide On Platinum Electrodes At Phosphate Buffer Solutions 1999:216.

[15] Badea M, Amine A, Palleschi G, Moscone D, Volpe G, Curulli A. New electrochemical sensors for detection of nitrites and nitrates. J Electroanal Chem 2001;509:66–72. doi:10.1016/S0022-0728(01)00358-8.

[16] Xiao P, Zhang Y, Garcia BB, Sepehri S, Liu D, Cao G. Nanostructured electrode with titania nanotube arrays: fabrication, electrochemical properties, and applications for biosensing. J Nanosci Nanotechnol 2009;9:2426–36. doi:10.1166/jnn.2008.SE21.

[17] Scheller F, Schubert F.MWCNT modified graphite electrode for electrochemical determination of BHA Biosensors. 1992.doi:10.1016/S0021-9673(01)93769-0.

[18] Sahraoui Y, Chaliaa S, Maaref A, Haddad A. An Electrochemical Nitrite Sensor Based on a Multilayer Film of Polyoxometalate 2013;2013:84–93.

[19] Arslan H .Service PH. Hydrogen peroxideJ Electroanal Chem 2001;509:66–72. doi:10.1016/S0022-0728(01)00358-8.

[20] Hayat A, Marty JL. Disposable screen printed electrochemical sensors: Tools for environmental monitoring. Sensors 2014;14:10432–53. doi:10.3390/s140610432.

[21] Farghaly O a, Hameed RSA, Abu-Nawwas A-AH. Analytical Application Using Modern Electrochemical Techniques. Int J Electrochem Sci 2014;9:3287–318.

[22] Arslan F, Ustabaş S, Arslan H. An amperometric biosensor for glucose determination prepared from glucose oxidase immobilized in polyaniline-polyvinylsulfonate film. Sensors 2011;11:8152–63. doi:10.3390/s110808152.

[23] Abramson SB, Attur M, Amin a R, Clancy R, Abstracts E, Achari Y, et al. Guide to soxhlet extraction. Osteoarthr Cartil 2012;8:1199–216. doi:10.1016/j.micinf.2011.07.011.Innate.

[24] Zhang Q, Fu S, Li H, Liu Y. A novel method for the determination of hydrogen peroxide in bleaching effluents by spectroscopy. BioResources 2013;8:3699–705.

[25] Cefic. Hydrogen Peroxide for industrial use Determination of hydrogen peroxide content Titrimetric method 2003:1–8.

[26] Yilong Z, Dean Z, Daoliang L. Electrochemical and other methods for detection and determination of dissolved nitrite: A review. Int J Electrochem Sci 2015;10:1144–68.

[27] Yoon I, Li JJJTJZ, Shim YK, Unep, Sutherland D (Aarhus U, Filipponi L (Aarhus U, et al. Drug Delivery. Drug Deliv 2008;51:1–19. doi:10.1016/j.micinf.2011.07.011.Innate.

[28] Lipfert J, Doniach S, Das R, Herschlag D. Understanding nucleic acid-ion interactions. vol. 83. 2014. doi:10.1146/annurev-biochem-060409-092720.

[29] Zhang ZZZ. Flexible camera calibration by viewing a plane from unknown orientations. Proc Seventh IEEE Int Conf Comput Vis 1999;1:0–7. doi:10.1109/ICCV.1999.791289.

[30] Razmi H, Heidari H. Amperometric determination of hydrogen peroxide on surface of a novel PbPCNF-modified carbon-ceramic electrode in acidic medium. J Electroanal Chem 2009;625:101–8. doi:10.1016/j.jelechem.2008.10.014.

[31] Sharon M, Soga T, Afre R, Sathiyamoorthy D, Dasgupta K, Bhardwaj S, et al. Hydrogen storage by carbon materials synthesized from oil seeds and fibrous plant materials. Int J Hydrogen Energy 2007;32:4238–49. doi:10.1016/j.ijhydene.2007.05.038.

[32] Ganesh V, Muthurasu a. Strategies for an enzyme immobilization on electrodes: Structural and electrochemical characterizations. J Phys Conf Ser 2012;358:12003. doi:10.1088/1742-6596/358/1/012003.

[33] Liu ZM, Yang Y, Wang H, Liu YL, Shen GL, Yu RQ. A hydrogen peroxide biosensor based on nano-Au/PAMAM dendrimer/cystamine modified gold electrode. Sensors

Actuators, B Chem., vol. 106, 2005, p. 394–400. doi:10.1016/j.snb.2004.08.023.

[34] Negahdary M, Asadi A, Mehrtashfar S, Imandar M, Akbari-Dastjerdi H, Salahi F, et al. A biosensor for determination of H_2O_2 by use of HRP enzyme and modified CPE with Zno Nps. Int J Electrochem Sci 2012;7:5185–94.

[35] Asaka K, Ottova A, Tien HT. Mediated electron transfer across supported bilayer lipid membrane (s-BLM). Thin Solid Films 1999;354:201–7. doi:10.1016/S0040-6090(99)00520-9.

[36] Lu X, Zhang Q, Zhang L, Li J. Direct electron transfer of horseradish peroxidase and its biosensor based on chitosan and room temperature ionic liquid. Electrochem Commun 2006;8:874–8. doi:10.1016/j.elecom.2006.03.026.

[37] Liu S, Ju H. Reagentless glucose biosensor based on direct electron transfer of glucose oxidase immobilized on colloidal gold modified carbon paste electrode. Biosens Bioelectron 2003;19:177–83. doi:10.1016/S0956-5663(03)00172-6.

[38] Wang G, Xu JJ, Chen HY, Lu ZH. Amperometric hydrogen peroxide biosensor with sol-gel/chitosan network-like film as immobilization matrix. Biosens Bioelectron 2003;18:335–43. doi:10.1016/S0956-5663(02)00152-5.

[39] Yin H, Ai S, Shi W, Zhu L. A novel hydrogen peroxide biosensor based on horseradish peroxidase immobilized on gold nanoparticles-silk fibroin modified glassy carbon electrode and direct electrochemistry of horseradish peroxidase. Sensors Actuators, B Chem 2009;137:747–53. doi:10.1016/j.snb.2008.12.046.

[40] Adrio JL, Demain AL. Microbial enzymes: tools for biotechnological processes.

Biomolecules 2014;4:117–39. doi:10.3390/biom4010117.

[41] Homaei AA, Sariri R, Vianello F, Stevanato R. Enzyme immobilization: An update. J Chem Biol 2013;6:185–205. doi:10.1007/s12154-013-0102-9.

[42] Datta S, Christena LR, Rajaram YRS. Enzyme immobilization: an overview on techniques and support materials. 3 Biotech 2012:1–9. doi:10.1007/s13205-012-0071-7.

[43] Tischer W, Wedekind F. Immobilized Enzymes: Methods and Applications. Biocatal Discov to Appl 1999;200:95–126. doi:10.1007/3-540-68116-7.

[44] Noe MC, Gilbert AM. Targeted Covalent Enzyme Inhibitors. Annu Rep Med Chem 2012;47:413–39. doi:10.1016/B978-0-12-396492-2.00027-8.

[45] Mateo C, Palomo JM, Fernandez-Lorente G, Guisan JM, Fernandez-Lafuente R. Improvement of enzyme activity, stability and selectivity via immobilization techniques. Enzyme Microb Technol 2007;40:1451–63. doi:10.1016/j.enzmictec.2007.01.018.

[46] Saleh Ahammad a J, Lee J-J, Rahman MA. Electrochemical sensors based on carbon nanotubes. Sensors (Basel) 2009;9:2289–319. doi:10.3390/s90402289.

[47] Rivas GA, Rubianes MD, Rodríguez MC, Ferreyra NF, Luque GL, Pedano ML, et al. Carbon nanotubes for electrochemical biosensing. Talanta 2007;74:291–307. doi:10.1016/j.talanta.2007.10.013.

[48] Lalwani G, Kwaczala AT, Kanakia S, Patel SC, Judex S, Sitharaman B. Fabrication and characterization of three-dimensional macroscopic all-carbon scaffolds. Carbon N Y 2013;53:90–100. doi:10.1016/j.carbon.2012.10.035.

[49] Ahammad AJS, Lee JJ, Rahman MA. Electrochemical Sensors Based on Carbon Nanotubes. Sensors 2009;9:2289–319. doi:Doi 10.3390/S90402289.

[50] Moore RR, Banks CE, Compton RG. Basal plane pyrolytic graphite modified electrodes: Comparison of carbon nanotubes and graphite powder as electrocatalysts. Anal Chem 2004;76:2677–82. doi:10.1021/ac040017q.

[51] Banks CE, Crossley A, Salter C, Wilkins SJ, Compton RG. Carbon nanotubes contain metal impurities which are responsible for the "electrocatalysis" seen at some nanotube-modified electrodes. Angew Chemie - Int Ed 2006;45:2533–7. doi:10.1002/anie.200600033.

[52] Chauke VP, Antunes E, Nyokong T. Comparative behavior of conjugates of tantalum phthalocyanines with gold nanoparticles or single walled carbon nanotubes towards bisphenol A electrocatalysis. J Electroanal Chem 2011;661:1–7. doi:10.1016/j.jelechem.2011.06.019.

[53] Zidan M, Tee TW, Abdullah AH, Zainal Z, Kheng GJ. Electrochemical Oxidation of Ascorbic Acid Mediated by Bi2O3 Microparticles Modified Glassy Carbon Electrode. Int J Electrochem Sci 2011;6:289–300.

[54] Siddiquee S, Yusof NA, Salleh AB, Tan GS, Bakar FA. Enhancement of dna immobilization and hybridization on gold electrode modified using zno nanoparticles/chitosan film. Curr Anal Chem 2011;7:296–305. doi:10.2174/157341111797183047.

[55] Periasamy AP, Ting SW, Chen S. Amperometric and Impedimetric H_2O_2 Biosensor

Based on Horseradish Peroxidase Covalently Immobilized at Ruthenium Oxide Nanoparticles Modified Electrode 2011;6:2688–709.

[56] Batra N, Tomar M, Gupta V. ZnO-CuO composite matrix based reagentless biosensor for detection of total cholesterol. Biosens Bioelectron 2015;67:263–71. doi:10.1016/j.bios.2014.08.029.

[57] Wang S, Xie F, Liu G. Direct electrochemistry and electrocatalysis of heme proteins on SWCNTs-CTAB modified electrodes. Talanta 2009;77:1343–50. doi:10.1016/j.talanta.2008.09.019.

[58] Mendoza-Huízar LH, Rios-Reyes CH, Gómez-Villegas MG. Zinc electrodeposition from chloride solutions onto glassy carbon electrode. J Mex Chem Soc 2009;53:243–7.

[59] Periasamy AP, Yang S, Chen S-M. Preparation and characterization of bismuth oxide nanoparticles-multiwalled carbon nanotube composite for the development of horseradish peroxidase based H_2O_2 biosensor. Talanta 2011;87:15–23. doi:10.1016/j.talanta.2011.09.021.

[60] Kaifer AE. Fundamentals of Analytical Chemistry. Sixth edition (Skoog, Douglas A.; West, Donald M.; Hollar, James F.). J Chem Educ 1992;69:A305. doi:10.1021/ed069pA305.1.

[61] Rahman ASMS, Islam MA, Shorowordi KM. Electrodeposition and Characterization of Copper Oxide Thin Films for Solar cell Applications. Procedia Eng 2015;105:679–85. doi:10.1016/j.proeng.2015.05.048.

[62] Sagu JS, Peiris TAN, Wijayantha KGU. Rapid and simple potentiostatic deposition of

copper (II) oxide thin films. Electrochem Commun 2014;42:68–71. doi:10.1016/j.elecom.2014.02.014.

[63] Nicholson RS. Theory and Application of Cyclic Voltammetry f m Measurement of Electrode Reaction Kinetics. Anal Chem 1965;37:1351–5. doi:10.1021/ac60230a016.

[64] DuVall SH, McCreery RL. Control of catechol and hydroquinone electron-transfer kinetics on native and modified glassy carbon electrodes. Anal Chem 1999;71:4594–602. doi:10.1021/ac990399d.

[65] Kissinger PT, Heineman WR. Cyclic voltammetry. J Chem Educ 1983;60:702. doi:10.1021/ed060p702.

[66] Brown JH. Development and Use of a Cyclic Voltammetry Simulator To Introduce Undergraduate Students to Electrochemical Simulations. J Chem Educ 2015;92:1490–6. doi:10.1021/acs.jchemed.5b00225.

[67] Settle F a. Handbook of Instrumental Techniques for Analytical Chemistry. Prentice Hall PTR 1997:968. doi:10.1109/MEI.1998.730821.

[68] Bard a, Faulkner L. Allen J. Bard and Larry R. Faulkner, Electrochemical Methods: Fundamentals and Applications, New York: Wiley, 2001. Russ J Electrochem 2002;38:1505–6. doi:10.1023/A:1021637209564.

[69] Streeter I, Thompson M, Compton RG. Linear sweep voltammetry at the tubular electrode: Theory of EC2 mechanisms. J Electroanal Chem 2006;591:133–40. doi:10.1016/j.jelechem.2006.03.043.

[70] Yuan Y, Wang L, Amemiya S. Chronoamperometry at micropipet electrodes for

determination of diffusion coefficients and transferred charges at liquid/liquid interfaces. Anal Chem 2004;76:5570–8. doi:10.1021/ac0493774.

[71] Orazem ME, Tribollet B. Electrochemical Impedance Spectroscopy. 2008. doi:10.1002/9780470381588.

[72] Ates M. Review study of electrochemical impedance spectroscopy and equivalent electrical circuits of conducting polymers on carbon surfaces. Prog Org Coatings 2011;71:1–10. doi:10.1016/j.porgcoat.2010.12.011.

[73] Manohar AK, Bretschger O, Nealson KH, Mansfeld F. The use of electrochemical impedance spectroscopy (EIS) in the evaluation of the electrochemical properties of a microbial fuel cell. Bioelectrochemistry 2008;72:149–54. doi:10.1016/j.bioelechem.2008.01.004.

[74] Liu M. Synthesis of ZnO Nanowires and Applications as Gas Sensors. Science (80-) 2010;1.

[75] Wang JX, Sun XW, Wei A, Lei Y, Cai XP, Li CM, et al. Zinc oxide nanocomb biosensor for glucose detection. Appl Phys Lett 2006;88. doi:10.1063/1.2210078.

[76] Shumba M, Nyokong T. Electrode modification using nanocomposites of boron or nitrogen doped graphene oxide and cobalt (II) tetra aminophenoxy phthalocyanine nanoparticles. Electrochim Acta 2016;196:457–69. doi:10.1016/j.electacta.2016.02.166.

[77] Thomas D, Thomas T, A JPP, E TJ, Augustine S. Electron Beam Irradiated ZnO Nanoparticles / Oxidized MWCNTs Modified GCE as a Supercapacitor 2015;10:7771–82.

[78] Montalbetti CAGN, Falque V. Amide bond formation and peptide coupling. Tetrahedron

2005;61:10827–52. doi:10.1016/j.tet.2005.08.031.

[79] Kolb HC, Finn MG, Sharpless KB. Click Chemistry: Diverse Chemical Function from a Few Good Reactions. Angew Chemie - Int Ed 2001;40:2004–21. doi:10.1002/1521-3773(20010601)40:11<2004::AID-ANIE2004>3.0.CO;2-5.

[80] Palanisamy S, Cheemalapati S, Chen SM. Highly sensitive and selective hydrogen peroxide biosensor based on hemoglobin immobilized at multiwalled carbon nanotubes-zinc oxide composite electrode. Anal Biochem 2012;429:108–15. doi:10.1016/j.ab.2012.07.001.

[81] Periasamy AP, Ting SW, Chen SM. Amperometric and impedimetric H2O2 biosensor based on horseradish peroxidase covalently immobilized at ruthenium oxide nanoparticles modified electrode. Int J Electrochem Sci 2011;6:2688–709.

APPENDIX

APPENDIX A: MATERIALS

List A1: Apparatus used for the study

Beakers, volumetric flasks, burette, spatula, sample bottles, funnels, measuring cylinders and syringes.

Table A.1: Reagents and chemicals

Name	Chemical formulae	Manufacturer	Concentration/mass
Distilled water	H_2O	MSU	-
Hydrogen peroxide	H_2O_2	ACE	0.001M
Hydrochloric acid	HCl	ACE	0.1M
Acetic acid	CH_3COOH	Cosmo chemicals	0.1M
Potassium ferricyanide	$K_3[Fe(CN)]_6$	ACE	10mM
Sodium hydroxide	NaOH	Skylabs	0.1M
Multiwalled carbon nanotubes	MWCNT	Sigma Aldrich	1mg/L
Ethanol	C_2H_5OH	Skylabs	99%
Di-potassium hydrogen phosphate	K_2HPO_4	Skylabs	17.41g

Zinc acetate dihydrate	$[Zn(O_2CCH_3)_2(H2O)_2]$	ACE	0.05M
Potassium chloride	KCl	ACE	1M
Sulphuric acid	H_2SO_4	ACE	0.1M

Table A.2: Instrumentation

Name	Model	Manufacturer	Use
Analytical Balance	GA-110	OHAUS	Weighing
pH meter	Az–8601	OHAUS	pH measurement
PGSTAT	PGSTAT302F	Autolab	Electrocatalysis
Ultra-Sonicator	KQ-250B	China Corp	Ultra agitation

Treatment of Glassware

Laboratory liquid soap was used for washing all glassware and they were rinsed using distilled water to remove contaminants and impurities.

APPENDIX B

B1: Surface area

Constant R = 8.314, T = 273 K

Randle-sevick equation

$I_p = (2.69 \times 10^5)n^{3/2}AD^{1/2}V^{1/2}C$

D= $7.6 \times 10^{-6} cm^2/s$, C= 1×10^{-6} cm^2, m=1×10^{-5} and A = $0.123\ cm^2$

B2: Limit of Detection and Limit of Quantification

Excel Linest function

Slope	**Intercept**
Standard error of the slope	Standard error of the intercept
R^2	Standard error in y

Limit of detection was 3.48 x 10^{-7} Mfor hydrogen peroxide

B3 Concentration studies

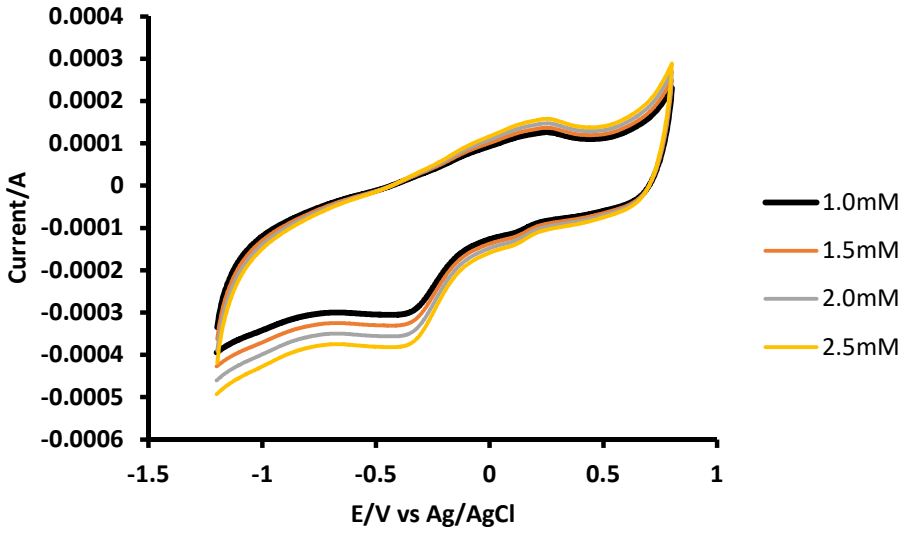

Voltammograms for HRP/ZnO/MWCNT/GCE in 0.1 M phosphate buffer solution (pH4.0) solution at 0.1 V/s at a potential of -1.2 to 0.6 V for different concentrations of hydrogen peroxide.